Benchmarking Flattening Filter-Free Photons for IMRT/VMAT Using TG119

By

Sarah Ashmeg

Graduate Program in Medical Physics
Duke University

Date: _____

Approved:

_____
Jennifer O'Daniel, Co-Supervisor

_____
Fang-Fang Yin, Co-Supervisor

_____
Timothy Turkington

Thesis submitted in partial fulfillment of
the requirements for the degree of Masters of Science in the Graduate Program in
Medical Physics of Duke University

2014

ABSTRACT

Benchmarking Flattening Filter-Free Photons for IMRT/VMAT using TG119

By

Sarah Ashmeg

Graduate Program in Medical Physics
Duke University

Date: _____

Approved:

_____
Jennifer O'Daniel, Co-Supervisor

_____
Fang-Fang Yin, Co-Supervisor

_____
Timothy Turkington

An abstract of a thesis submitted in partial
fulfillment of the requirements for the degree
of Masters of Science in the Graduate Program in
Medical Physics of Duke University

2014

Abstract

TG119 is a report published by The American Association of Physicists in Medicine (AAPM) to be used for Intensity Modulated Radiation Therapy (IMRT) commissioning. Nine institutions contributed to TG119 by creating and delivering five IMRT cases of varying complexity. Each institution measured the dose of each plan and formed a confidence limit (CL) such that CL = |mean| + 1.96 SD. The given confidence limits form a baseline for other institutions to be used in IMRT commissioning. However, since the publication of TG119 in 2009, new techniques have emerged in the field of radiation therapy including Volumetric Arc Therapy (VMAT) and the Flattening Filter Free (FFF) mode in advanced linear accelerators. Our goal in this work is to verify the feasibility of using TG119 to commission VMAT and FFF systems and to set a benchmark for other institutions to use.

We created 48 plans of the five sites given in TG119 in addition to a "real" head and neck (HN) case. For each site, we planned IMRT and VMAT using 6 MV and 10 MV, Flattening Filter (FF) and FFF modes (6x2x2x2 = 48 plans). All our plans were created on the Eclipse treatment planning system (Varian Medical Systems, Palo Alto, CA) and delivered on three beam-matched TrueBeam linear accelerators (Varian Medical System) at Duke University Medical Center.

Measurements were taken using an ion chamber, films, and a pseudo-3D diode array (Delta4), and compared to the planned doses. Confidence limits were determined using the approach of TG119 (CL = |average mean deviation| + 1.96 SD). We used the student's paired t-test to determine any statistically significant differences between IMRT and VMAT, FF and FFF for 6 MV and 10 MV.

The majority of the ion chamber measurements (94%) agreed with the planned doses to within 3%. The majority of errors > 3% involved the HN IMRT plans, either TG119 or "real". For film measurements, we used gamma parameters of 3%, 3mm with a 20% threshold. All films met an acceptability criterion of <= 10% of pixels failing gamma. As for Delta4, gamma parameters of 3%, 3mm with a 5% threshold were used. All plans met the acceptability criterion of 90% of pixels passing (average 99.7% +/- 0.8%). A second analysis was performed using 2%, 2mm gamma parameters, wherein almost all plans met the 90% passing rate criterion (average 98.9% +/- 2.5%).

Confidence limits were established for ion chamber (3.1%), film (6%), and Delta4 (3.1%) measurements. All the confidence limits were comparable to TG119 institutions. We recommend that non-clinical plans (e.g. 10 MV HN plans) not be included in TG119 evaluations. We also recommend that film continue to be used as the gold standard of multi-dimensional measurements, rather than be replaced by diode-based technology.

Dedication

To my parents, siblings and friends for their continuous support. To Chris for his valuable help and encouragement and to Ferris for being my motivation.

Contents

Abstract iv

List of Tables x

List of Figures xi

Acknowledgements xiii

1.Introduction 1

1.1 Linear Accelerators 1

1.1.1 The Traditional Design 1

1.1.2 Flattening-Filter Free Mode 3

1.2 Radiation Delivery Modalities 6

1.2.1 3D Conformal 6

1.2.2 IMRT 7

1.2.3 VMAT 10

1.3 Radiation Measurement Devices 10

1.3.1 Ionization Chambers 10

1.3.2 Films 12

1.3.3 3D Dosimetry 14

1.4 TG119 16

1.5 Hypothesis 21

2. Materials and Methods 22

2.1 Plans 23

2.1.1 AP-PA 23
2.1.2 Bands 23
2.1.3 Multitarget 25
2.1.4 Cshape 26
2.1.5 Prostate 26
2.1.6 TG119 Head and Neck 26
2.1.7"Real" Head and Neck Case 27
2.2 Measurements Analysis 28
3. Results 31
3.1. Planning Results 31
3.2. Bands: Film Measurements 31
3.3. Site-specific Cases: Measurements Results 32
3.3.1. Ion Chamber Results 32
3.3.2. Film Results 42
3.3.3. Delta4 Results 45
3.4. P_{ion} Effect 52
3.5. High Dose Rate Effect 53
4. Discussions 55
4.1. Planning Results 55
4.2. Bands Results 55
4.3. Test Cases 55
4.3.1. Ion Chamber 55

4.3.2. Film 58

4.3.3. Delta4 58

5. Conclusions 60

Appendix A 61

References 69

List of Tables

Table 1: Comparison of Measured Confidence Level for 6 MV vs. 10 MV, FF vs. FFF, and IMRT vs. VMAT with and without the 10 MV HN Measurements 39

Table 2: Statistical Differences for VMAT vs. IMRT, FFF vs. FF, and High vs. Low Dose Region Ion chamber Measurements Based on the Student's Paired T-Test..... 41

Table 3: Statistical Differences for VMAT vs. IMRT, FFF vs. FF, and High vs. Low Dose Region 6MV Film Measurements Based on the Student's Paired T-Test 45

Table 4: Gamma 3%, 3mm Passing Points Percentage for all Plans of all Energies 46

Table 5: Gamma 2%, 2mm Passing Points Percentage for all Plans of all Energies 47

Table 6: Confidence Limits (% Pixels Failing Gamma) for 3%, 3mm and 2%, 2mm Gamma Criteria 48

Table 7: Statistical Differences for VMAT vs. IMRT and FFF vs. FF 3D Measurements Based on the Student's Paired T-Test 49

Table 8: Statistical Comparison of 2% / 2mm Gamma Analysis of 3D Data 50

Table 9: Film – Delta4 Data Correlation..... 51

Table 10: P_{ion} Values for 6 MV and 6 MV FFF with the Chamber Inserted in Different Depths..... 53

Table 11: Ion Chamber Measurement vs. Planned Results..... 54

List of Figures

Figure 1: A simplified diagram of a LINAC.....3

Figure 2: 10 MV beam profile (left) vs. 10 MV FFF beam profile (right).....5

Figure 3: Isodose lines in the Multitarget plan 7

Figure 4: A diagram presenting MLCs: (a) Parked. (b) Shaped to deliver a small dose through a window in IMRT.....8

Figure 5: 0.01 cc ion chamber (left) and a 0.6 cc Farmer chamber (right).....11

Figure 6: Electrometer 12

Figure 7: A radiographic film with an IMRT dose delivered 14

Figure 8: Delta4, a pseudo 3D QA device.....15

Figure 9: A screen capture from the Delta4 software showing the two panels and the analysis. 16

Figure 10: MultiTarget from Eclipse.....17

Figure 11: Prostate from Eclipse 18

Figure 12: TG119 Head and Neck from Eclipse.....19

Figure 13: Cshape from Eclipse.....20

Figure 14: Dose profile for the bands plan from Eclipse 24

Figure 15: A coronal view for MultiTarget 6 MV IMRT plan with isodose lines 25

Figure 16:"Real" head and neck case from Eclipse 27

Figure 17: IMRT cases for 6 MV with flattening filter, high dose regions (first 6 sites to the left) and low dose regions (7 sites to the right) 33

Figure 18: VMAT cases for 6 MV with flattening filter, high dose regions (first 6 sites to the left) and low dose regions (7 sites to the right) 34

Figure 19: IMRT cases for 6 MV flattening filter free (FFF), high dose regions (first 6 sites to the left) and low dose regions (7 sites to the right) 34

Figure 20: VMAT cases for 6 MV flattening filter free (FFF), high dose regions (first 6 sites to the left) and low dose regions (7 sites to the right) 35

Figure 21: IMRT cases for 10 MV with flattening filter free, high dose regions (first 6 sites to the left) and low dose regions (7 sites to the right) 35

Figure 22: VMAT cases for 10 MV with flattening filter free, high dose regions (first 6 sites to the left) and low dose regions (7 sites to the right) 36

Figure 23: IMRT cases for 10 MV flattening filter free (FFF), high dose regions (first 6 sites to the left) and low dose regions (7 sites to the right) 36

Figure 24: VMAT cases for 10 MV flattening filter free (FFF), high dose regions (first 6 sites to the left) and low dose regions (7 sites to the right) 37

Figure 25: Confidence levels of different TG119 institutions in high dose regions and low dose ones 38

Figure 26: Confidence levels of different energies and modes in high dose regions and low dose ones in our study 38

Figure 27: Confidence levels of different energies and modes in high dose regions and low dose ones of our study excluding the head and neck cases for 10 MV and 10 MV FFF 39

Figure 28: A high dose region comparison between film data for 6 MV, 6 MV FFF and TG119 institutions 42

Figure 29: A low dose region comparison between film data for 6 MV, 6 MV FFF and TG119 institutions 43

Figure 30: Mean % pixels failing gamma comparing TG119 institutions and measured data 44

Figure 31: Confidence limit (% pixels failing gamma) comparing TG119 institutions and measured data 44

Figure 32: Correlation between film results and Delta4 results 51

Acknowledgements

I ‘m sincerely grateful for the continuous support and advice I receive from Dr Yin, Dr O’Daniel, Dr Turkington and faculty, staff and students of the medical physics department at Duke University.

1. Introduction

1.1 Linear Accelerators

1.1.1 The Traditional Design

Linear accelerators accelerate charged particles using electric fields in the direction of the particles' propagation [1]. The charged particles are electrons produced by heating a filament. By applying a voltage, these electrons are guided to enter a waveguide. Simultaneously, an electric field enters the waveguide from an RF wave source, and the waves accelerate the electrons until a desired kinetic energy is achieved. In radiotherapy clinics, the electrons' energies are in the MeV range. These high-energy electrons can be used directly for treatment or to produce x-ray beams. Photons are produced when the electrons strike a tungsten target. In MeV energy range, the produced photons are mainly in the forward direction as opposed to keV beams where the probability of x-ray direction is similar in all angles.

Conventionally, in order to produce an adequate coverage throughout the tumor volume, a flattening filter is inserted in the photon beam's path. The flattening filter is a conic shape high Z material. The photons exit this filter with a homogeneous fluence (as measured at a depth of 10 cm in a water phantom) but varying mean energy across the plane. The beam has a higher mean energy (i.e. "harder" spectrum) in the center and lower mean energy (i.e. "softer" spectrum) towards the beam edges. In shallow depths,

however, this property is seen as horns at the sides of a beam profile and a dip in the center, but at a certain depth the profile becomes flat.

Below the target and the flattening filter, there are two sets of jaws to collimate the beams. In Varian (Varian Medical Systems, Palo Alto, CA) linear accelerators, the upper jaws are Y1 and Y2, which move towards the gantry or away from it when the collimator's angle is at zero. Below them are the X1 and X2 jaws which move in the perpendicular direction (left – right when the collimator is at zero angle). In modern VARIAN linear accelerators, a set of multi-leaf collimators (MLCs) is inserted under the X jaws. These MLCs move in the same direction as the lower jaws. The MLCs used in this study are Varian's Millennium-120, which are formed of 120 leaves equally divided between two banks (Bank A and Bank B). They are sized such that the projection at 100 cm from the source would be 5 mm thick for the central 40 leaves and 1 cm for the remaining 10 on each side within a bank. The MLCs are used to shape the beam to achieve high conformity around the tumor volume while shielding the surrounding tissue and organs at risk from photons. More recently, these MLCs have been developed to modulate the intensity within an open beam. This beam modulation is achieved by varying the location and speed of the MLCs within the treatment fields. Dose rate has units of MU/min where MU stands for Monitor Units. In radiotherapy, the monitor unit is a representation of the machine's output. This output is defined when the machine is

commissioned and is calibrated periodically. The output is monitored by a set of ion chambers above the jaws.

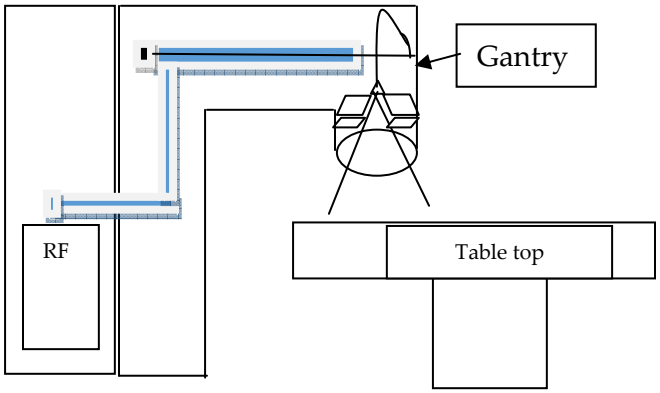

Figure 1: A simplified diagram of a LINAC

1.1.2 Flattening-Filter Free Mode

In the megavoltage energy range, X-rays are produced from the target in a forward direction relative to the direction of electrons incident upon the target [1]. Flattening filters have typically been inserted in the beam path in order to produce a uniform intensity across the field at a given depth, thereby providing a uniform dose. The removal of the flattening filter produces a beam with significant photon fluence (i.e. number of photons per cm^2) variation across the field and lower average photon energy. A comparison of the beam profile of flattened and un-flattened fields is shown in Figure 2. The higher photon fluence along the central axis allows for a high dose delivery rate, shortening patient treatment time. The lower photon fluence off-axis reduces out-of-field dose to normal tissue. The out-of-field dose is further lowered by the reduction of head

scatter from the linear accelerator due to both the removal of the flattening filter from the beam path (no scatter will occur within the flattening filter) and by the lower average photon energy. By reducing the out-of-field dose, the patient's risk of a secondary cancer induction is also lowered.

In our experience, the ideal treatment site for FFF beams is a small tumor (4cm diameter or less) prescribed to receive a high dose per fraction. As the tumor is small, the photon fluence does not vary significantly across the field. Therefore only minor field modulations with MLCs are required to produce good dosimetry. With minor modulations the MU increase is minimal. Therefore a large reduction in treatment time can be achieved. As the size of the tumor increases, the required MLC modulation to produce a flat field of adequate size increases along with the MU per field. The treatment of large tumors would not be appropriate for a FFF beam.

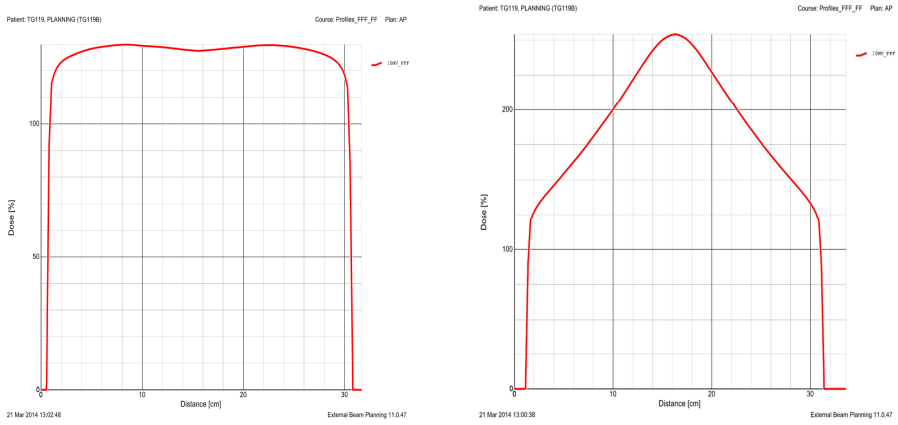

Figure 2: 10 MV beam profile (left) vs. 10 MV FFF beam profile (right)

Due to the reduced average energy and photo-neutron fluence in comparison to flattened beams, the same vaults can be used for FFF beams. The clinical physicist should remember that for FFF beams the conventional definition of flatness and symmetry might not be applicable [9]. The flatness for a flattened beam is typically measured at depths of d_{max} and 10 cm in water.

As a new technology in radiotherapy treatment delivery, it is important to fully verify the FFF commissioning. We have tested the quality assurance procedures used for FF radiation by TG119 to see if they may also be implemented for FFF radiation.

1.2 Radiation Delivery Modalities

1.2.1 3D Conformal

Computerized tomography (CT) and MLCs made the ability to conform the beam to the tumor volume while shielding the organs at risk from the main radiation beam achievable. Varian introduced their commercial MLCs in 1990 to the European and American markets [26]. By setting each leaf at a certain location the beam can be shaped around the tumor for each treatment angle. This is known in radiation oncology clinics as 3D conformal radiation therapy (3D CRT). The 3D CRT steps are as following:

a. Image the patient with a high quality 3D imaging device (typically CT). In this step the patient's setup and the choice of immobilization devices take place.
b. Contour the tumor volume and critical organs.
c. On a computer-based treatment planning system (TPS), create a treatment plan.
d. Calculate the dose to the tumor and organs at risk using an accurate dose calculation algorithm. We used the Analytical Anisotropic Algorithm (AAA) in our study.
e. Evaluate the plan using dose volume histograms (DVHs) which describe how much of a structure receives a given dose. In addition to DVH, isodose lines are used for plan evaluation. Isodose lines are lines that connect between points receiving an equal dose, as shown in Figure 3.

f. For treatment, the patient is placed in position then imaged using either kV or MV imaging. The patient's position is adjusted as needed prior to treatment.

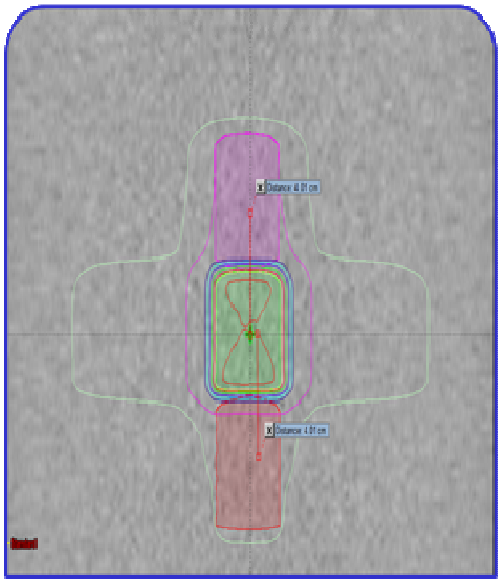

Figure 3: Isodose lines in the Multitarget plan

1.2.2 IMRT

Intensity-modulated radiation therapy (IMRT) increases the radiotherapy complexity beyond 3D-CRT by adding intensity modulation within each field. In 3DCRT planning, the beams are set at chosen angles with the use of compensators and MLCs to conform the beam around the tumor. The needed MUs to deliver the desired dose are calculated by the TPS. This is known as forward planning as opposed to inverse planning. In inverse planning, we set the dose goals for each structure (tumor volumes and organs at risk). Through an optimization process, the computer finds the plan that

best matches the given criteria. In each calculated field, the beam is modulated giving a variable intensity profile.

One way to modulate the beam's intensity is by varying the MLCs position within a field. There are two classes of MLC-based IMRT, step-and-shoot and sliding-window. For step-and-shoot delivery of a treatment field, the MLCs shift into different patterns in-between the beam turning on. In other words, the MLCs do not move while radiation is being delivered. For sliding-window delivery, the MLCs move while the beam is on. In both methods, the beam is off while the gantry moves to the next angle to deliver the following field. The sliding-window technique is also known as dynamic MLC delivery. Each pair of leaves would start at the same end and move in the same direction [1].

In the Varian linear accelerators we have used, the MLCs used are Millinnium 120. This MLC system by Varian is formed of 120 leaves (60 pairs). The central 40 pairs are 5 mm wide and the width of the remaining 20 pairs are 10 cm. These widths are of the projection at 100 cm from the target.

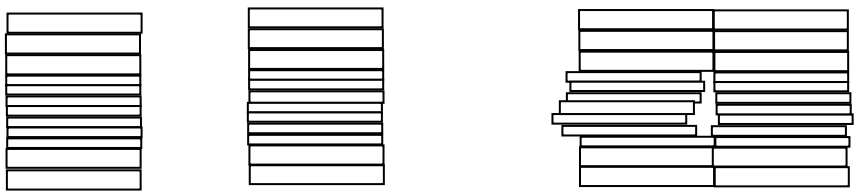

Figure 4: A diagram presenting MLCs: (a) Parked. (b) Shaped to deliver a small dose through a window in IMRT

The steps for IMRT planning are similar to 3D CRT in addition to the following:

a) Treatment beams are typically 5 to 9 equally-spaced beams.
b) Set dose constraints to target volumes and organs at risk.
c) The planning system creates a fluence map using an optimization method.
d) TPS performs a leaf motion calculation (to find the machine's ability to achieve the optimized fluence).
e) The treatment planner evaluates the 3D dose distribution and re-optimizes the plan as necessary.

In IMRT delivery, most of the beam is blocked by the multi-leaf collimator. Due to this fact, an error in MLC positioning can impact the dose distribution. Therefore, the accuracy of the MLC positioning and the stability of the leaf speed has to be tested periodically. In addition to that, a patient-specific QA has to be performed. In patient-specific QA, we create a verification plan by copying the patient's plan into a phantom and calculate the corresponding dose. This plan is then delivered to the phantom and a comparison between the TPS estimated dose and the measurement is used for analysis.

1.2.3 VMAT

The concept of Volumetric Modulated Arc Therapy (VMAT) was first introduced in 1995, but wasn't commercially available until after 2008 [5]. In VMAT, the gantry is no longer static but rotates while the radiation is delivered. Additionally, in VMAT the dose rate and gantry speed may be varied along with MLC leaf position. These additional variables increase the complexity of radiation treatment delivery above that of IMRT, highlighting the importance of adequate quality assurance techniques [6], [7].

In VMAT the beam delivery is fast and with lower MUs in comparison to conventional IMRT. The gantry can perform a full rotation in 60-65 seconds, varying based on the manufacturer. During an arc, the MLCs keep moving back and forth to deliver the desired photon fluence at all angles (as opposed to one direction motion in conventional DMLC). Also, during the beam's delivery, the dose rate varies.

1.3 Radiation Measurement Devices

1.3.1 Ionization Chambers

Ionization chambers (or ion chambers) are the most commonly used dosimetric devices in the radiation therapy clinics. Ion chambers are formed of enclosed gas (typically air) within a thin wall. When the radiation hits the chamber, the air gets ionized and a potential difference is applied between the anode and cathode. As a result,

the produced ions migrate to the electrode of opposite charge. The collected charges form an electric current proportional to the radiation dose.

The chamber of our choice is a thimble chamber, the most commonly used chamber in radiotherapy. Thimble chambers are cylindrically shaped with the wall being grounded and the applied potential on the central electrode. One of the most popular thimble chambers is the Farmer chamber. The Farmer chamber has a sensitive volume of 0.6 cc filled with air enclosed in graphite wall. However, smaller thimble chambers have been developed for small fields measurements. The miniature chambers are suitable for measurements in high gradient regions as well. Figure 5 shows a picture of a Farmer chamber and a 0.01 cc ion chamber.

The electron current collected by the chamber is displayed using an electrometer. Typically, the electrometer supplies the chamber with voltage and displays the measured charge or current. The chambers are connected to the electrometer using low-noise triaxial cables.

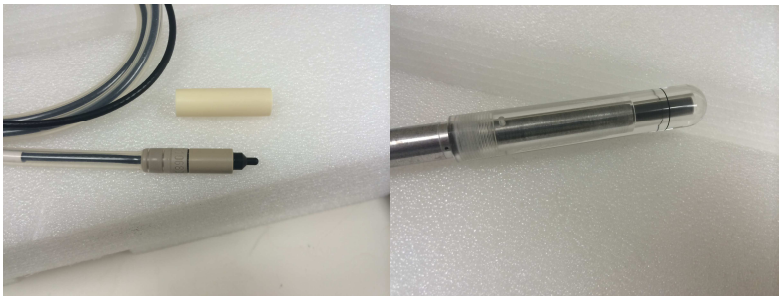

Figure 5: 0.01 cc ion chamber (left) and a 0.6 cc Farmer chamber (right)

Figure 6: Electrometer

1.3.2 Films

Films are usually used for qualitative analysis or for relative dosimetry [1], [26]. The main advantage of films is their high two-dimensional resolution information. Radiographic films consist of radiation-sensitive silver-halide crystals, which are sandwiched between gelatin emulsion coatings on both sides of the film. The emulsion provides the film with stiffness for film handling and stability against heat and chemical effects.

When the incident photons hit the crystal lattice, they generate electrons via photoelectric, Compton scatter or pair-production interaction. The electrons get trapped in impurities where they attract silver ions to form silver atoms after they combine. For the grain to be developable, it has to contain at least three silver atoms. The radiation forms a latent image on the film, which is later rendered by developing the film using chemicals.

The amount of the black silver molecules is proportional to the radiation dose. After irradiation and processing, the opacity of a region in the film is used as indication of the radiation's dose. Higher doses result in regions of higher opacity. The light opacity is defined as I_0 / I, where I_0 is the intensity of light without the film and I is the intensity of the light after passing through the film. In the clinic we use the optical density (OD), which is $\log_{10}$ of the opacity.

When films are used for dosimetry, a calibration curve has to be created for each used batch. The curve relates the OD to the radiation doses. Film dosimetry is becoming less popular in clinics due to the difficulty of maintaining film processors. With the movement towards digital imaging in both radiation and diagnostic clinics, many film processors have been removed or neglected.

Radiochromic films are a relatively recent development of film technology. Radiochromic films are insensitive to room light and do not need a film processor. These characteristics make them easy to use and convenient for relative dosimetry.

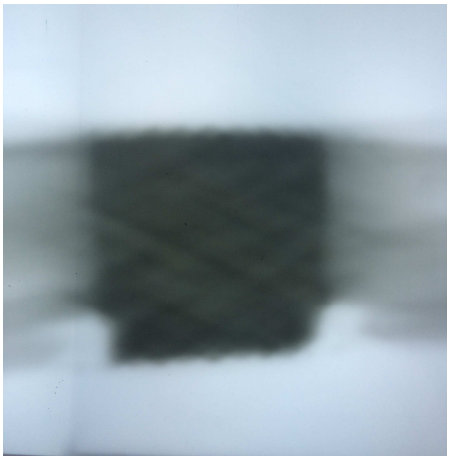

Figure 7: A radiographic film with an IMRT dose delivered

1.3.3 3D Dosimetry

Ionization chambers provide point dosimetry and films display planar dose. Delta4 is a pseudo 3D QA device composed of two planes of diode arrays crossing each other with a cylindrical phantom of PMMA (poly-methyl methacrylate) filling the space in between them. This phantom is 40 cm long and 22 cm in diameter. The planes consist of 1069 p-type silicon diodes with 0.039 mm^3 cylindrical sensitive volume and are arranged such that they are 5 mm away from each other in the center (6 cm x 6 cm area) and 1 cm apart in the remainder of the 20 cm x 20 cm panel. The data is measured by the detector arrays while the regions between them are estimated by interpolation. Hence it is a pseudo 3D device.

The Delta4 calibration is done by removing the panels from the PMMA phantom and then placing them in a rectangular acrylic phantom. The central diode is then

calibrated against an ion chamber. During calibration, the ion chamber has its own PMMA phantom. First the ion chamber measurement is taken with a field size of 10 x 10 cm^2. Then it (and its phantom) is removed from the beam, and one of the diode planes is placed into the beam for calibration. The other diodes are calibrated relatively to the central one, with the field size increased to encompass them. In order to calibrate the diodes in a stable beam, the arrays are irradiated and then moved in directions perpendicular to the beam several times [4].

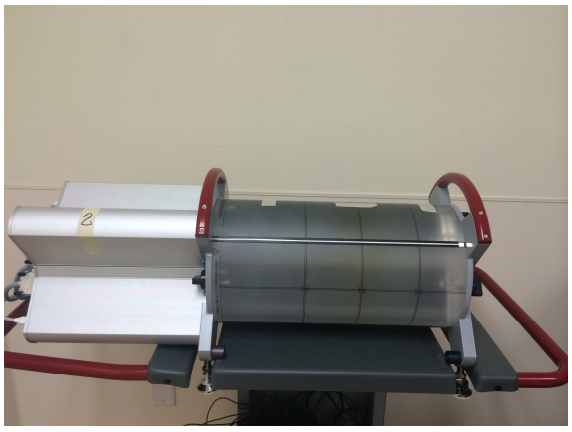

Figure 8: Delta4, a pseudo 3D QA device

The detector arrays are shown in Figure 9 with the blue dots being the points passing the gamma criteria while the reds dots are failing points.

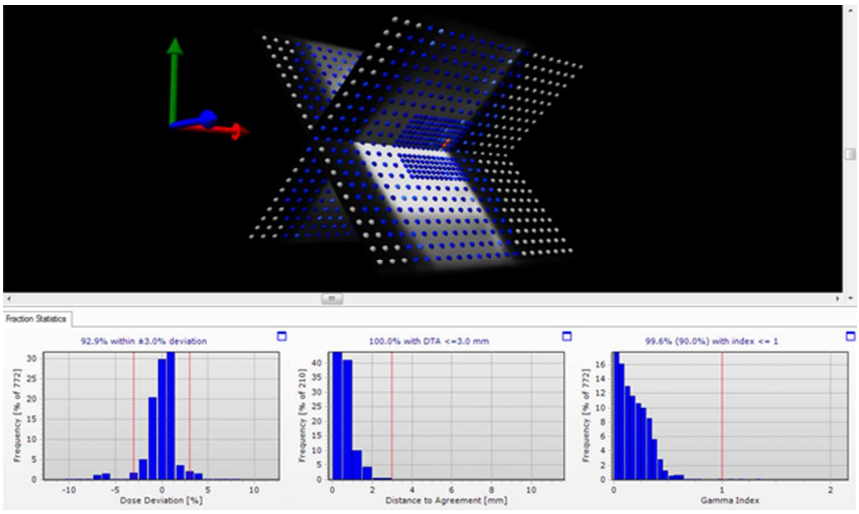

Figure 9: A screen capture from the Delta4 software showing the two panels and the analysis.

Delta4 provides more points of measurement in comparison to ion chamber (point dose) or film (planar dose) methods, therefore its results might be more representative of the entire dose distribution's accuracy.

1.4 TG119

The AAPM Task Group 119 [2] published their report in 2009 to set a benchmark for IMRT commissioning. This task group was formed after the Radiologic Physics Center (RPC) reported that 28% of the institutions involved failed the head and neck (HN) IMRT process. They produced a set of test cases in order to evaluate the IMRT treatment chain from simulation to delivery; these tests were for five different sites in addition to two preliminary tests.

The non-IMRT preliminary tests were a simple AP-PA open field and a series of AP-PA open fields of different sizes, used to create a stair-step dose pattern, which were given for calibration and to show the reliability of the assessment system for non-IMRT cases. These are followed by 5 IMRT plans of various complexity: multitarget, prostate, head-and-neck, and two Cshape targets with an internal avoidance structure.

The multitarget structures are formed of three cylinders, 4 cm in length and 4 cm in diameter. The superior, central, and inferior structures are supposed to receive 50%, 100%, and 25% of the target dose respectively. Planning goals are specified using D99 and D10 (dose to 99% and 10% of the volume respectively) to the three cylinders. The plan is composed of seven IMRT fields that are at 50° intervals from the AP. The ion chamber measurements take place in the center of each target (with applying 4.0 cm superior and inferior shifts), while the film data is collected mid-phantom.

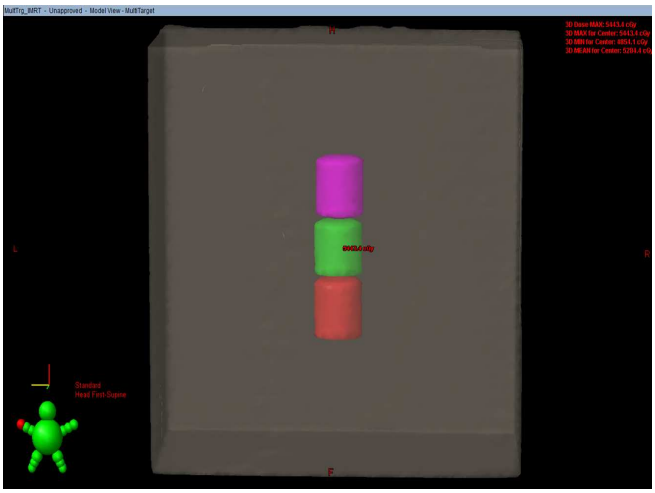

Figure 10: MultiTarget from Eclipse

The prostate CTV is an ellipsoid of the following dimensions: 4.0 cm right-left, 2.6 cm anterior-posterior and 6.5 cm superior-inferior. The PTV consists of the CTV plus a 0.6 cm isotropic margin. The bladder and rectum are the organs-at-risk. The planning goals are achieved using D95 and D5 for the prostate PTV, and using D30 and D10 for the organs at risk. The plan is composed of 7 fields, as in the multitarget case, which are at 50° intervals from the vertical. Measurements take place at the center of the PTV (the isocenter) and 2.5 cm posterior in the rectum.

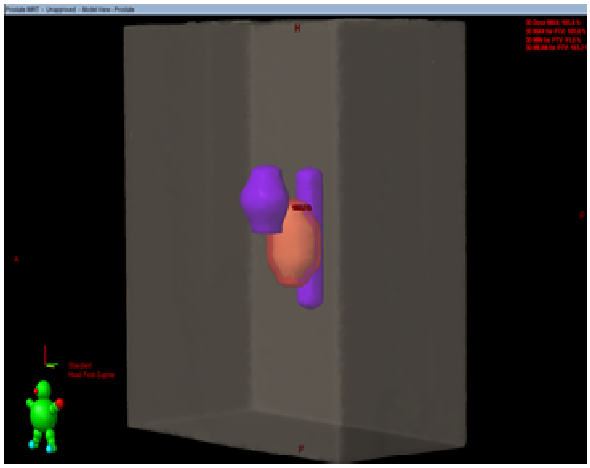

Figure 11: Prostate from Eclipse

The TG119 HN consists of a large PTV that extends from the base of the skull to upper neck. It is 0.6 cm away from the skin and 1.5 cm away from the spinal cord, which, along with the parotid glands, is an avoidance structure. The dose goals are

specified by D95, D90 and D20 for the PTV, D50 for the parotids and maximum dose for the cord. This plan was made with nine fields in 40° intervals from the AP, with the measurements taken in the PTV (the isocenter) and 4.0 cm posteriorly in the center of the cord. The film measurements show the dose to the parotid glands in mid-phantom measurements.

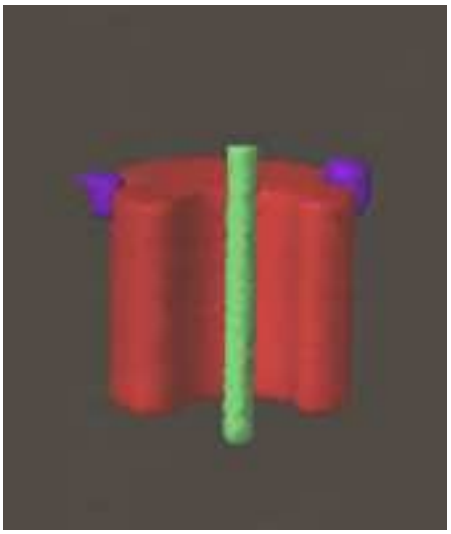

Figure 12: TG119 Head and Neck from Eclipse

Cshape is an 8 cm long C-shaped target with an inner radius of 1.5 cm and an outer radius of 3.7 cm. This PTV surrounds a central 10 cm long - 1 cm radius cylindrical core with a 0.5 cm gap between the core and the PTV. This time, however, the isocenter is placed in the avoidance structure instead of the PTV such that the low dose / high gradient region is in the isocenter. One of the cases is easy with achievable goals in which the core gets 50% of the target dose. In the second one (hard), the core is

supposed to be kept to only 20% of the target dose. The goal of the hard plan is to test the limits of the planning and delivery system, as it is practically impossible to achieve. The dose goals are specified by D95 and D10 for the PTV and by D10 for the OAR. The beam arrangements are the same for both plans. They are composed of 9 fields that are in 40° intervals from the AP. Measurements take place in the isocenter (central core) and 2.5 cm anteriorly in the PTV for both ion chamber and films.

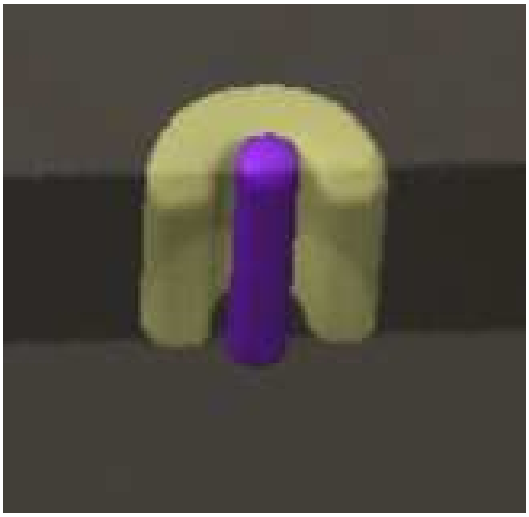

Figure 13: Cshape from Eclipse

These structures are available on the AAPM website and can either be downloaded or drawn by the individual into the TPS. Following the planning and measurements steps given in the TG119, other institutions can verify their IMRT commissioning by comparing their confidence limit (CL) values to the TG119 values, where CL = |mean| + 1.96 SD.

The TG119 institutions used different treatment planning systems and machines depending on the availability to the institution. They all planned and delivered IMRT plans using 6 MV beams because it was the only energy available to all institutions. However, since the publication of TG119, new techniques have emerged in the field of radiation oncology. Some have become widely used, such as VMAT and FFF. In this work we study the feasibility of using TG119 to commission VMAT and FFF using two different energies (6 MV and 10 MV).

1.5 Hypothesis

In this study, we introduce two hypotheses. The first is that TG119 IMRT cases can be re-purposed for (1) VMAT commissioning and for (2) flattening-filter free (FFF) beam commissioning. The second hypothesis states that the pseudo-3D diode QA device (Delta4) will provide similar results to film. To test the first hypothesis, the results of the TG119 methodology will be compared between IMRT/VMAT, FF/FFF, and this study/TG119 institutions. To test the second hypothesis, the Delta4 measurements will be compared to film measurements.

2. Materials and Methods

We followed the TG119 recommendations for planning and choice of phantoms. All structures are available in a DICOM format and can be downloaded from the AAPM website, http://www.aapm.org/pubs/tg119/default.asp. Alternatively, the structures can be contoured manually if preferred by the planner.

We used a 0.01 cc chamber with a depth of 7.5cm in a solid water phantom to acquire point measurements of different plans. We also compared some of the 0.01 cc chamber measurements to 0.1 cc chamber measurements for investigation and obtained similar results. We used the 0.01cc chamber, however, for its better resolution in the low dose region.

We CT scanned a 30x30x15 cm^3 phantom with an insert for a CC01 ion chamber, and another one with no insert but of same dimensions for film measurements. The phantom consisted of solid water slabs of different thicknesses such that the ion chamber (or the film) was at a depth of 7.5 cm. In addition to the 0.01 cc ion chamber (point measurement) and EDR2 (Extended Dose Range) film measurements (2D), we used a pseudo3D diode device (Delta4, ScandiDos, Uppsala, Sweden). The homogeneous cylindrical phantom CT image provided by the vendor was used for dose calculations, as is done clinically.

All treatment plans and dose calculations were done in Eclipse v 10.0.39 and were delivered at the TrueBeam machines at Duke University Medical Center using an

Aria record-and-verify system (Varian Medical Systems, Palo Alto, CA). The calculation grid in these plans was 2.5mm in all cases. Eight plans for each energy and each technique were created, yielding a total of eight preliminary plans (AP-PA and bands for 6 MV, 6 MV FFF, 10 MV and 10 MV FFF) and forty eight site-specific plans (6 sites, IMRT and VMAT, 6 MV, 6 MV FFF, 10 MV and 10 MV FFF).

2.1 Plans

2.1.1 AP-PA

This test is done in order to convert the MUs to dose per field while also eliminating the daily output fluctuations. It consists of two fields Anterior-Posterior (AP) and Posterior-Anterior (PA) of 10x10 cm^2 field size. 200 cGy/ fraction (100 cGy / field) was delivered to the isocenter and was measured with the ion chamber. The open field AP-PA measurement in the isocenter was done to establish the cGy/nC for the ion chamber during the measurement session (i.e. to obtain a conversion factor that relates the charges measured by the ion chamber into dose in cGy).

2.1.2 Bands

Five open fields of various sizes were used to deliver a stair-step dose pattern across a 15cm field. The X jaws were fixed to a 15 cm opening, with Y_1 set at +7.5 cm and with Y_2 varying from -4.5 cm to +7.5 cm. The bands are made to test the film QA ability

which makes this test useful for film calibration. We used our own film calibration plan developed at Duke.

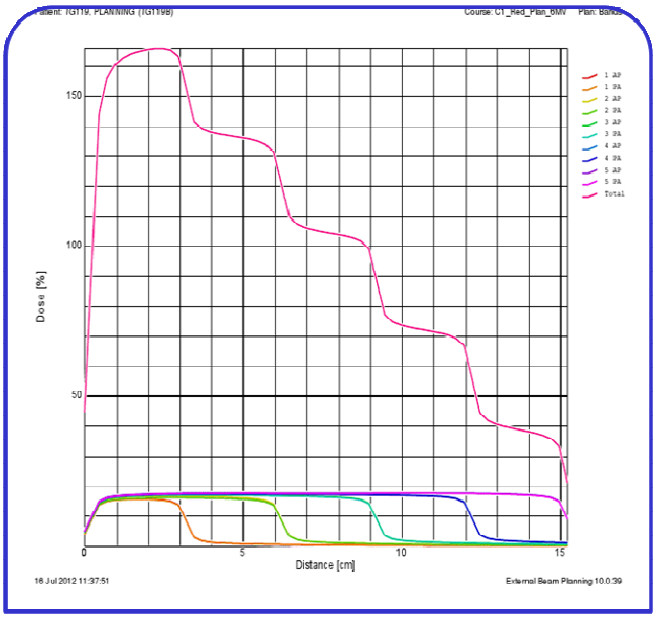

Figure 14: Dose profile for the bands plan from Eclipse

In Figure 14, the upper curve (the one that looks like stairs from side) is the accumulated dose from all 10 fields, while the lower curve is the contribution from each band. Each one of the five bands is composed of two fields an AP and a PA, thus we have a total of 10 fields.

2.1.3 Multitarget

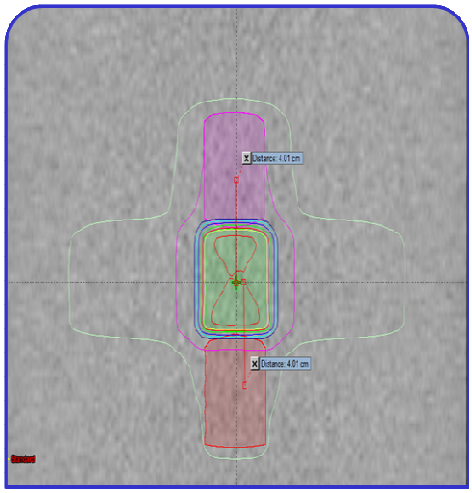

Figure 15: A coronal view for MultiTarget 6 MV IMRT plan with isodose lines

For the multitarget case, the IMRT plans consisted of seven beams at angles given by TG119 (0^o, 100^o, 150^o, 310^o, 260^o and 210^o). Each field delivered around 30 cGy/ fraction to give a total dose of around 210 cGy/ fraction to the isocenter. In the VMAT plans, we used a single arc to deliver the dose.

The ion chamber measurements take place in the center of each target. The isocenter is in the middle of the central target and then we apply two shifts to the centers of the other two cylinders and measure. The film measurement is taken only in mid-plane since the shifts are in a superior-inferior (sup – inf) direction.

2.1.4 Cshape

For this site, we created two plans that vary in complexity. One is simple (easy) and the other is difficult (hard) with impossible constraints. The purpose of the hard one is to test the upper limits of the system. In the easy plan, the core is supposed to get 50% of the target dose while the hard plan aims for 20%.

The beam arrangements for the IMRT plans are 9 beams at 40 degree intervals from the AP beam. For VMAT plans, the Cshape easy had one arc (360 degrees) while the hard one consisted of two arcs. The measurements took place at the center of the core for the ion chamber and mid-plane for films. We then applied a 2.5 cm shift anteriorly to measure at the high dose/low gradient region in the target.

2.1.5 Prostate

This test mimics a prostate case with the rectum being the organ at risk of interest. The isocenter is the center of the PTV while the mid-rectum is 2.5 cm posterior to isocenter. Both ion chamber and film measurements are taken at isocenter and 2.5 cm posteriorly. The IMRT plan was composed of seven fields at 0^{o}, 50°, 100^{o}, 150^{o}, 310^{o}, 260^{o} and 210^{o}. We used a single arc for the VMAT plans.

2.1.6 TG119 Head and Neck

The IMRT plans, in this case, consist of nine beams at 40 degree intervals from the AP field while the VMAT plan had two arcs. The ion chamber measurements are taken at the isocenter (mid PTV) and 4.0 cm posteriorly at the center of the cord. Film

measurements were acquired at mid-phantom, including both PTV and parotids, and at 4.0 cm posteriorly for cord measurements.

2.1.7"Real" Head and Neck Case

The ion chamber measurement results for 10 MV and 10 MVFFF TG119 HN failed to meet an action level of less than 3% error. As a result we chose an actual "real" patient case that was treated at Duke University Medical Center and performed the tests on it. The IMRT beams were at the following angles: 180, 140, 100, 60, 20, 340, 300, 260 and 220 degrees, and the VMAT plans had two arcs. The isocenter measurements were in the PTV (or mid-plane for films) and then a posterior shift was taken for low dose region measurements.

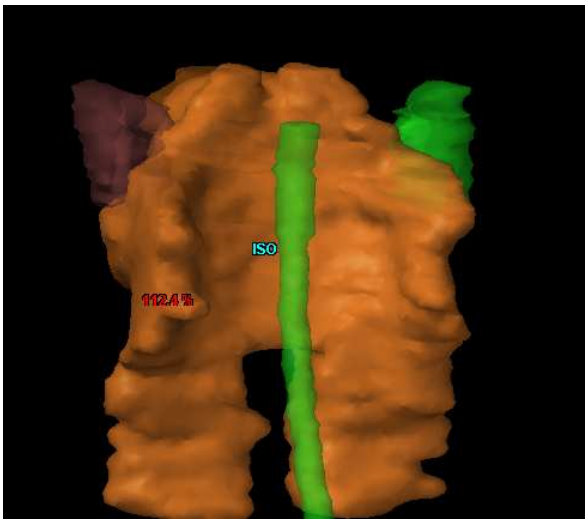

Figure 16:"Real" head and neck case from Eclipse

2.2 Measurements Analysis

We compared our measurements to the planned doses using a 0.01 cc ion chamber for point measurements, films for 2D and Delta4 for 3D analysis. We also calculated the confidence levels, as described below, for each method and compared them to each of the TG119 institutions' confidence levels. This requires comparing each of 6 MV IMRT, 6 MV FFF IMRT, 6 MV VMAT, 6 MV FFF VMAT, 10 MV IMRT, 10 MV FFF IMRT, 10 MV VMAT and 10 MV FFF VMAT to the TG119's 6 MV IMRT results. The paired student's t-test was used to determine the statistical significance between IMRT and VMAT, 6 MV and 10 MV energies and FF and FFF. The Delta 4 results were compared in a pass/fail fashion to the ion chamber results for all plans. Gamma criteria were set for 3% dose difference (DD) and 3mm distance to agreement (DTA), global gamma. In addition to the above, we analyzed film data for 6 MV and 6 MV FFF and compared them to the film results given by the six film contributing institutions of TG119.

For ion chamber measurement analysis, we compared our measured doses to the planned doses, [error = (measured – planned) / Rx]. EDR2 films were used for the planar analysis of IMRT and VMAT plans for 6 MV and 6 MV FFF energies. The films were inserted and exposed at a depth of 7.5 cm in a solid water phantom and then compared against a calibration film. Unlike the TG119 method where they normalized to ion chamber measurements in a corresponding point or area, we matched between

measurement and plan in a high dose-low gradient region to get a relative comparison. We used a Vidar (Vidar Systems Corporations, Herndon, VA) scanner to scan the films and then used the OmniPro software (IBA Dosimetry, Schwarzenbruck, Germany) to analyze them. Films were analyzed using gamma index. The gamma index is a quantitative description of how well the measured planar dose matches the planned dose. The index is composed of two variables: the dose difference between measured and planned values at a given point (DD, chosen here to be 3%) and the distance to agreement (DTA, chosen to be 3mm) which is the distance between a measured point and the closest point in the plan that exhibits equal dose [24]. The pseudo 3D measurements were also analyzed using the gamma index, with criteria of 3%, 3mm with 5% threshold.

In addition, we used the confidence level (CL) as defined and recommended by TG119. The CL for a group of measurements is given by CL = | mean | + 1.96 SD. The formula accounts for both systematic errors (in the mean deviation) and random errors (in the standard deviation). The calculated CL encompasses roughly 97.5% of the data, assuming an even distribution about the mean. TG119 used the data of all institutions as its input for determining an overall CL that any individual institution should be able to achieve. In our study, we calculated a CL for a variety of measurement groupings (all IMRT measurements, all FFF measurements, all 6 MV measurements) to use to compare the accuracy and stability of a variety of treatment delivery methods. For ion chamber

measurements, the mean deviation was the percentage-error between measurement and planned doses. For film and Delta4 measurements, the mean deviation was the percentage of pixels failing to meet the gamma criteria.

3. Results

3.1. Planning Results

Tables A through D in Appendix A show the planning goals for each site along with our planning results in comparison to TG119 institutions and whether the goals are achieved within two standard deviations of the TG119 institutions.

All planning results achieved the goals set by TG119 ± 2 standard deviation, with the exception of 6 MV FFF VMAT plans. The PTV and Core D10 of Cshape easy and Core D10 in Cshape hard, specifically, failed to meet the criteria. In addition, the 10 MV FFF "real" HN VMAT plan did not meet the PTV's D20 TG119 criteria. However, the planning for this case was from a real case that has been treated at Duke University Hospital and the constraints were not set based on TG119.

3.2. Bands: Film Measurements

The points passing gamma criteria for 6 MV and 6 MV FFF are 98.90% and 98.81% respectively. The analysis for this test, as well as for other film data, was done relative to the planned plane by matching a point in high dose/low gradient region in the measured plane to a similar point in the plan. We did not measure the central dose using an ion chamber while acquiring the films.

3.3. Site-specific Cases: Measurements Results

We collected data for six sites using ion chamber and Delta4 (MultiTarget, Cshape easy, Cshape hard, TG119 HN, "real" HN case and Prostate) using all combinations of 6 MV/10MV, IMRT/VMAT and FF/FFF. Film measurements were done for the five cases given by TG119 using IMRT and VMAT for energies 6 MV and 6 MV FFF.

3.3.1. Ion Chamber Results

a) Measured Dose vs. Planned Dose

The results of ion chamber measurements are shown in Figures 17 to 24. These results represent the error which must be within 3% to pass. The error represents the discrepancy between our planned doses and measured doses, with error is defined as error = (measured dose – planned dose)/prescribed dose. The figures show the %error for each energy and mode in each case. Each figure includes the average of the TG119 institutions with the error bars being 2 standard deviations as given by the TG119 report.

The majority of the ion chamber measurements (94%) agreed with the planned doses to within 3%. The majority of errors > 3% involved the HN IMRT plans, either TG119 or "real". All 6 MV & 6 MV FFF measurements had errors <= 3%, except for one 6 MV FFF with an error of 3.3% (TG119 HN IMRT). All 10 MV measurements were within 3% of planned doses except for one deviation (-5.7%, TG119 HN IMRT).The majority of

the discrepancies were found with 10 MV FFF IMRT plans, three of which involving HN IMRT plans (-3.2%, -4.9%, -3.3%) and one involving the Cshape Hard plan (+3.8%). All failing measurements were confirmed by re-measuring with ion chamber.

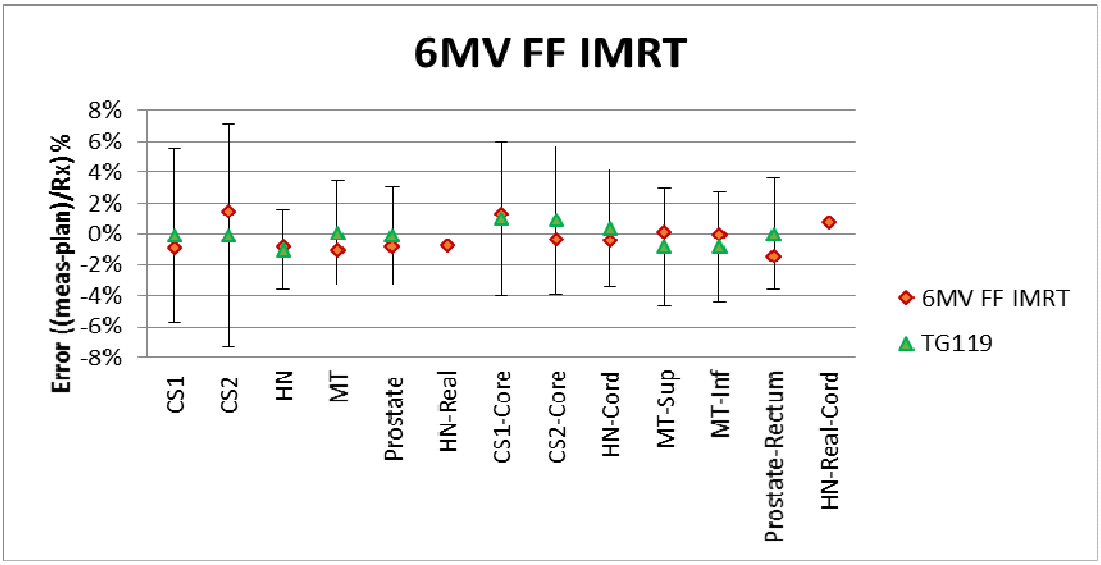

Figure 17: IMRT cases for 6 MV with flattening filter, high dose regions (first 6 sites to the left) and low dose regions (7 sites to the right)

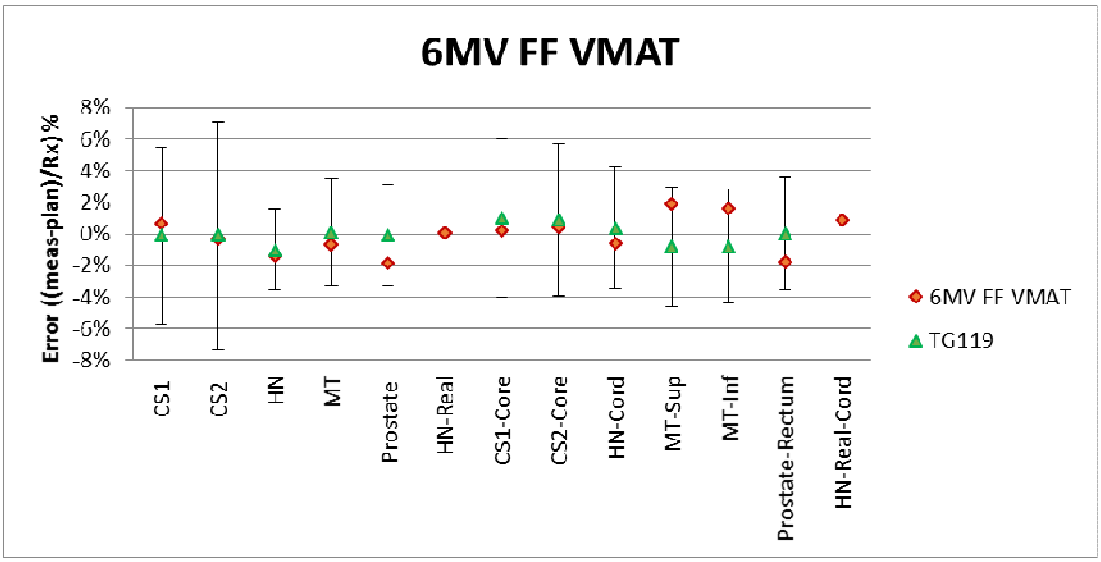

Figure 18: VMAT cases for 6 MV with flattening filter, high dose regions (first 6 sites to the left) and low dose regions (7 sites to the right)

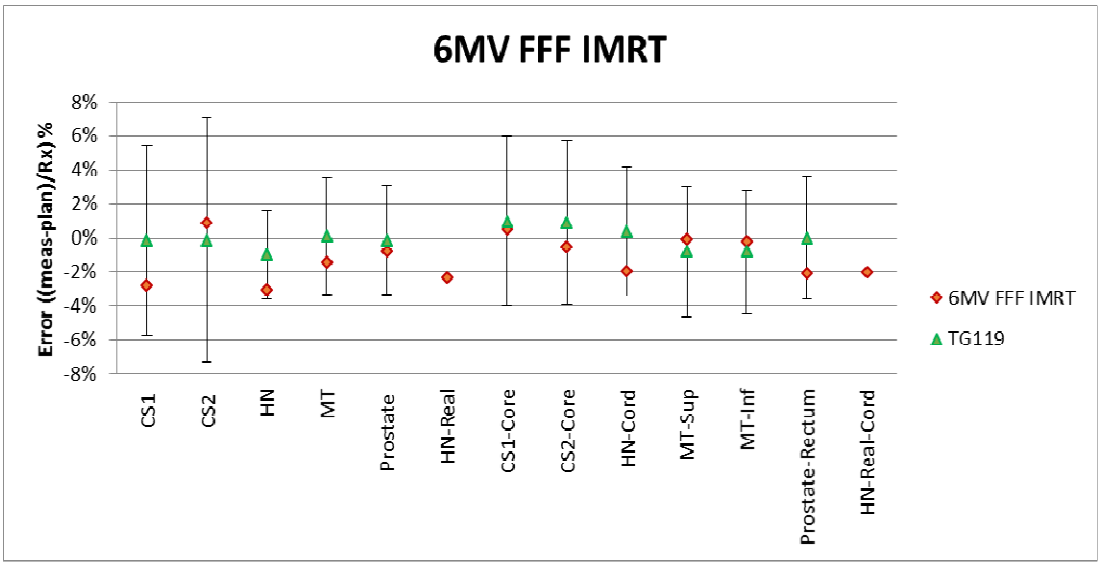

Figure 19: IMRT cases for 6 MV flattening filter free (FFF), high dose regions (first 6 sites to the left) and low dose regions (7 sites to the right)

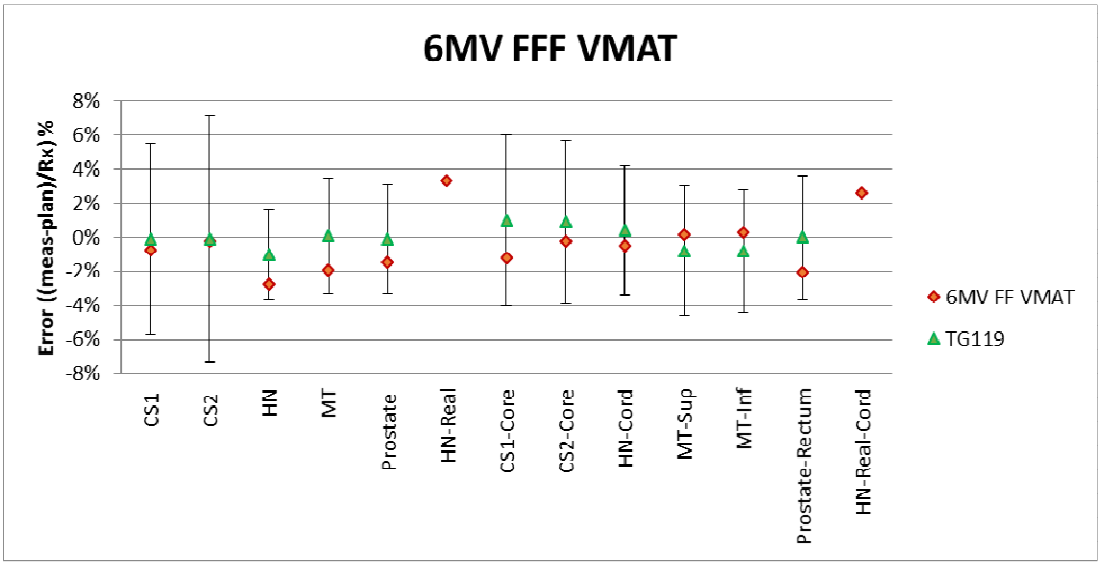

Figure 20: VMAT cases for 6 MV flattening filter free (FFF), high dose regions (first 6 sites to the left) and low dose regions (7 sites to the

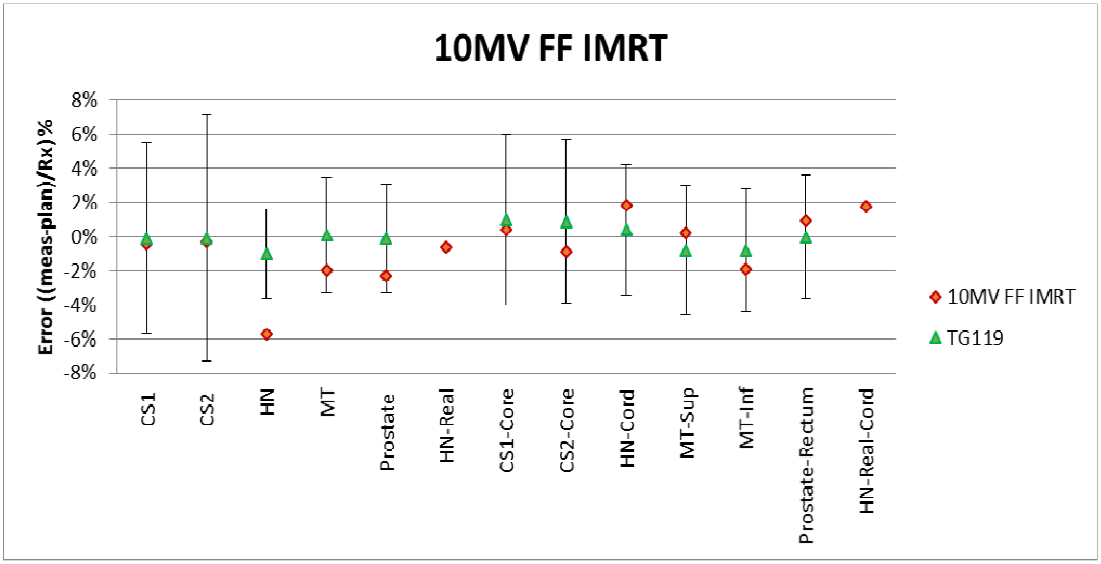

Figure 21: IMRT cases for 10 MV with flattening filter free, high dose regions (first 6 sites to the left) and low dose regions (7 sites to the right)

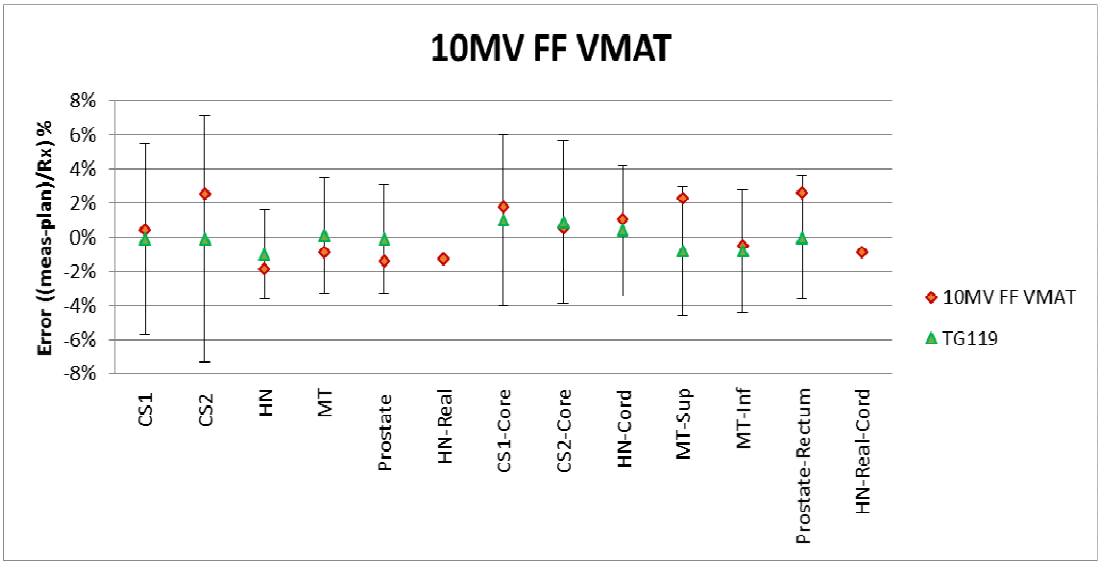

Figure 22: VMAT cases for 10 MV with flattening filter free, high dose regions (first 6 sites to the left) and low dose regions (7 sites to the right)

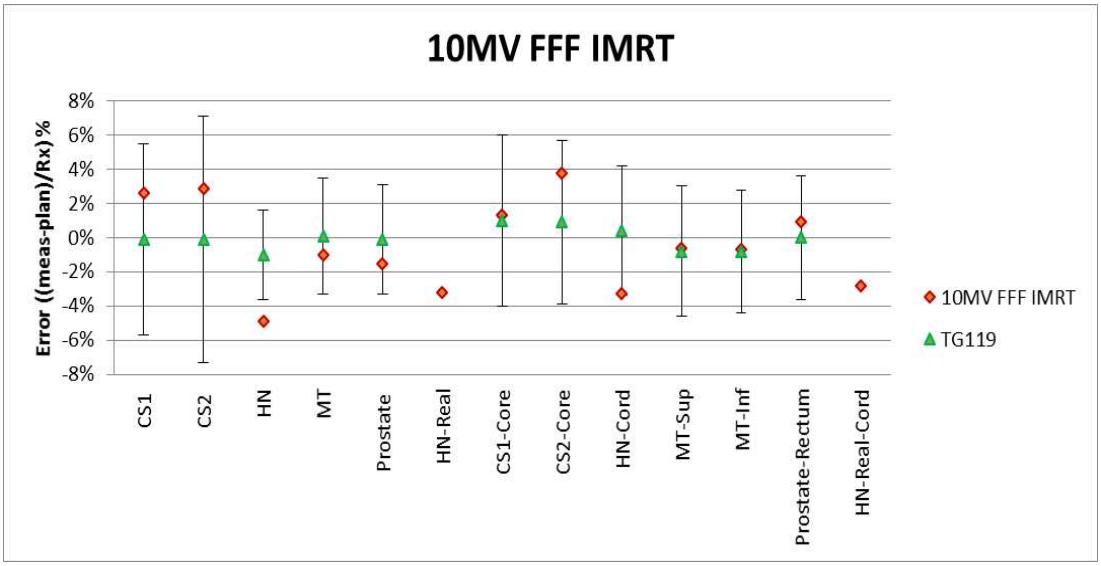

Figure 23: IMRT cases for 10 MV flattening filter free (FFF), high dose regions (first 6 sites to the left) and low dose regions (7 sites to the right)

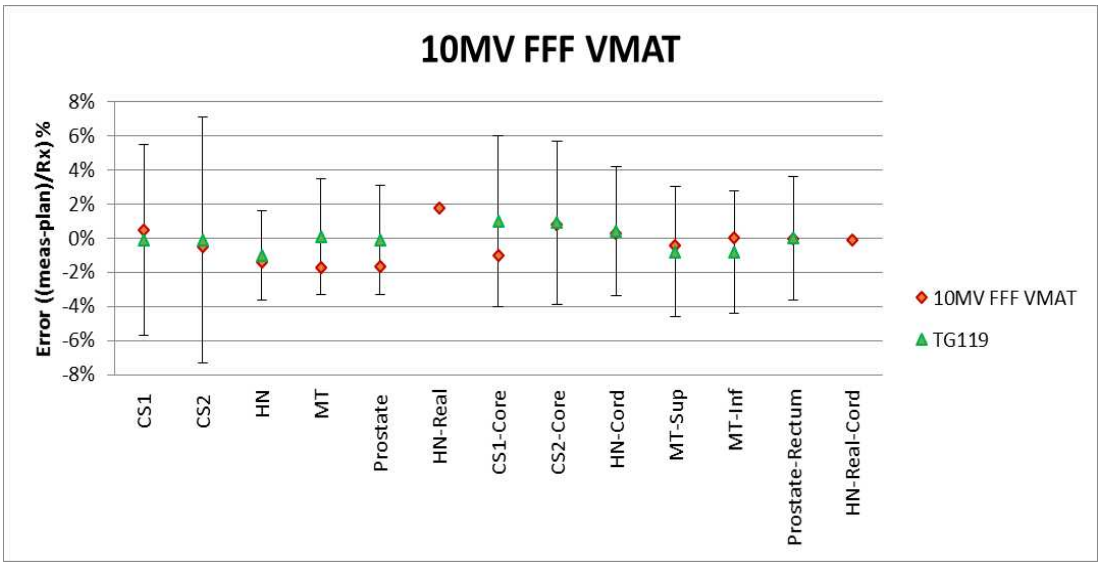

Figure 24: VMAT cases for 10 MV flattening filter free (FFF), high dose regions (first 6 sites to the left) and low dose regions (7 sites to the right)

b) Measured Data vs. TG119

In figures 10 through 17 we present our measurements in comparison with the TG119 institutions measurements for each plan. All ion chamber measurements agreed with the (mean + 2SD) from TG119 except for the 10 MV IMRT TG119 HN plan (both FF and FFF). In addition, we calculated the confidence level, defined previously as CL = |mean|+1.96SD, and compared the measured results to the TG119 institutions as shown in Figures 25, 26 and 27; and Table 1.

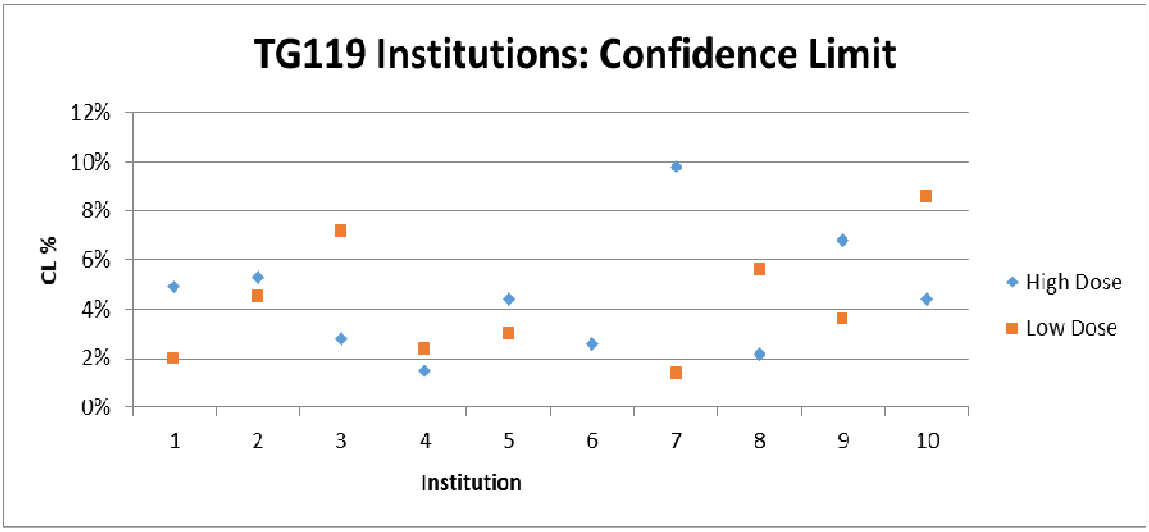

Figure 25: Confidence levels of different TG119 institutions in high dose regions and low dose regions

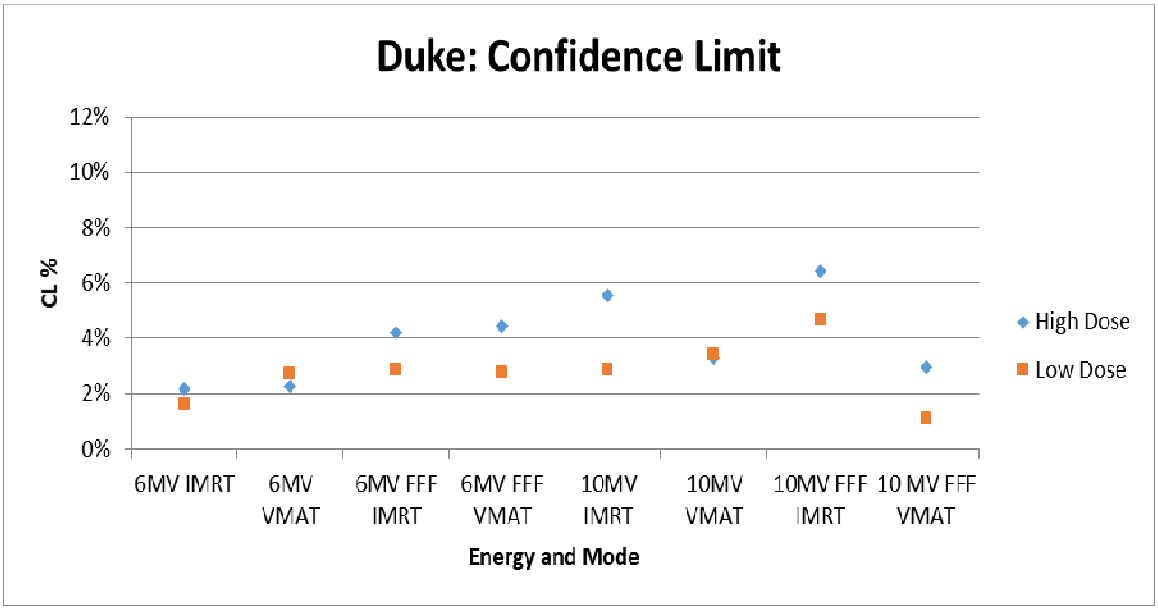

Figure 26: Confidence levels of different energies and modes in high dose regions and low dose regions in our study

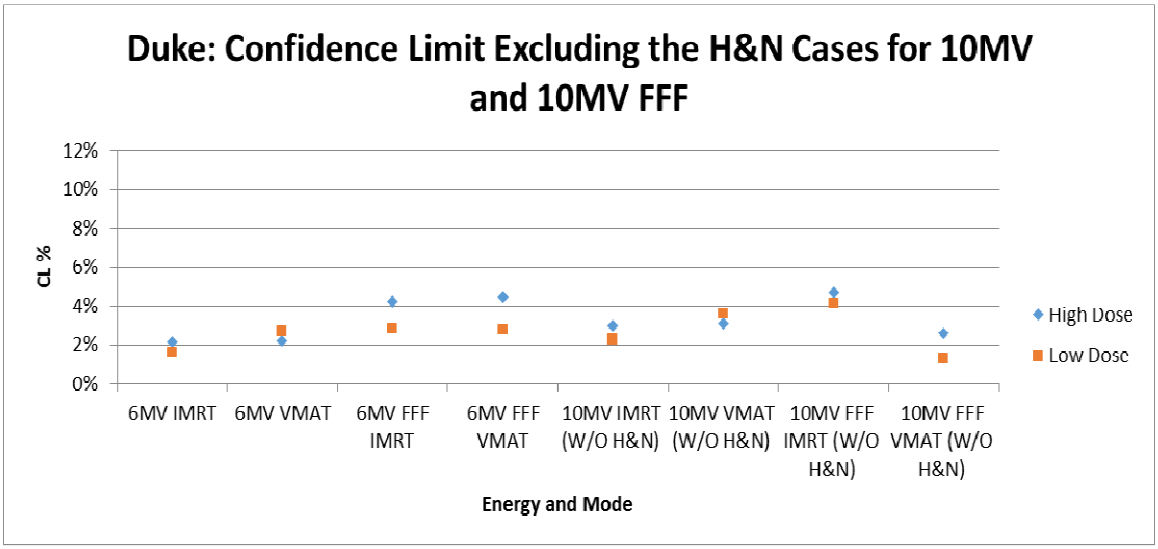

Figure 27: Confidence levels of different energies and modes in high dose regions and low dose regions of our study excluding the head and neck cases for 10 MV and 10 MV FFF

Table 1: Comparison of Measured Confidence Level for 6 MV vs. 10 MV, FF vs. FFF, and IMRT vs. VMAT with and without the 10 MV HN Measurements

	Confidence Limit	
All IC measurements	3.5%	
All IC excluding 10 MV HN	3.1%	
	6 MV	**10 MV**
All ion chamber measurements	3.5%	4.7%
All IC excluding 10 MV HN	3.5%	3.3%
	FF	**FFF**
All ion chamber measurements	3.7%	4.5%
All IC excluding10 MV HN	2.8%	4.0%

	IMRT	VMAT
All ion chamber measurements	4.2%	2.8%
All IC excluding 10 MV HN	3.3%	2.9%
	High Dose Region	**Low Dose Region**
All ion chamber measurements	4.1%	2.9%
All IC excluding 10 MV HN	3.4%	2.7%

c) Statistical Analysis

We used the student's paired t-test to find the p-values and evaluate the statistical significance of VMAT vs. IMRT, FFF vs. FF and high dose region vs. low dose region. This paired t-test uses the null hypothesis, assuming that the mean of the population of difference scores across the two measurements is zero. This would indicate that there is no statistically significant difference between the two groups being tested. We separated our data into many groupings, sorting by energy (6 MV & 10 MV), delivery technique (IMRT & VMAT), & machine design (FF & FFF). The groupings share from the same data population. For example, the second row of Table 2 compares VMAT vs. IMRT for 6 MV plans. This particular analysis compares all 6 MV VMAT plans (both FF and FFF) against all 6 MV IMRT plans (both FF and FFF). The third row compares FF vs. FFF for 6 MV plans. This analysis then separates the data into 6 MV FF

plans (both VMAT and IMRT) and 6 MV FFF plans (both VMAT and IMRT). This pattern is continued throughout Table 2.

Table 2: Statistical Differences for VMAT vs. IMRT, FFF vs. FF, and High vs. Low Dose Region Ion chamber Measurements Based on the Student's Paired T-Test

Energy	**N (number of data pairs)**	**Tests**	**p-value**	**Statistically Significant**
6 MV	24	VMAT vs. IMRT	0.221	No
	24	FFF vs. FF	0.022	Yes
	24	High vs. Low	0.059	No
10 MV	24	VMAT vs. IMRT	0.358 (0.949 w/o HN)	No
	24	FFF vs. FF	0.894 (0.500 w/o HN)	No
	24	High vs. Low	0.004 (0.015 w/o HN)	Yes
6 MV and 10 MV	48	VMAT vs. IMRT	0.046 (0.212 w/o 10 MV HN)	Yes (No)
	48	FFF vs. FF	0.099 (0.193 w/o 10 MV HN)	No
	48	High vs. Low	0.002 (0.008 w/o 10 MV HN)	Yes

3.3.2. Film Results

As in TG119, we did a composite plan delivery and comparison (not field by field) with the coronal film plane at isocenter. We applied shifts to the HN, Cshape, and prostate plans to measure a second coronal plane per TG119.

a) Measured Dose vs. Planned Dose

We analyzed the films using gamma criteria of 3% DD, 3mm DTA and 20% threshold (figures 28 and 29). The 20% threshold was selected based on the lowest dose point measured by the calibration film. The only exception was the two prostate-shifted film measurements, which used a 40% threshold to eliminate contamination from the processor. All films met the acceptability criteria of <= 10% of pixels failing gamma.

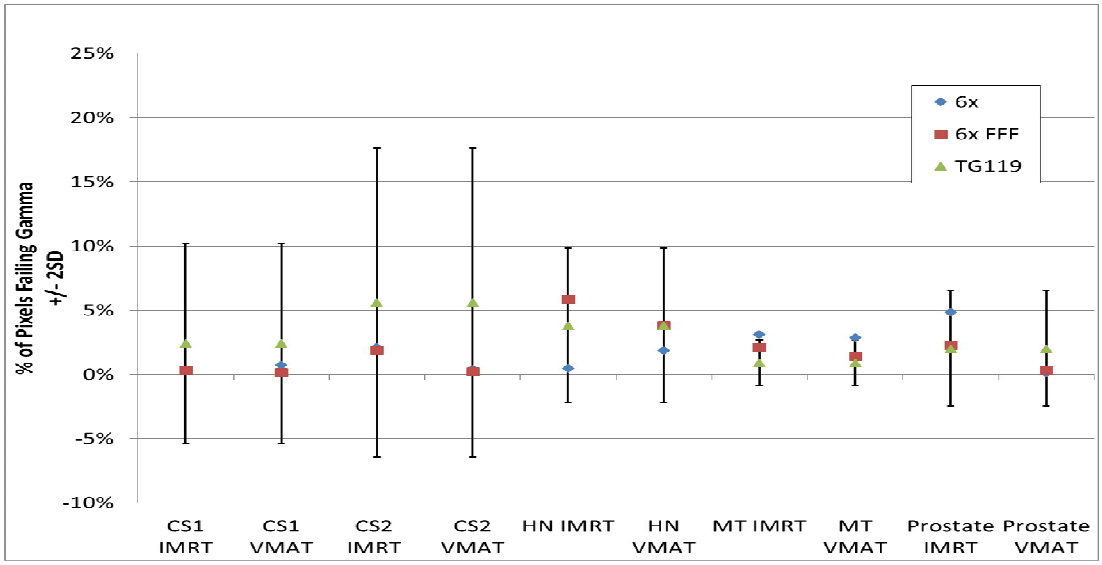

Figure 28: A high dose region comparison between film data for 6 MV, 6 MV FFF and TG119 institutions

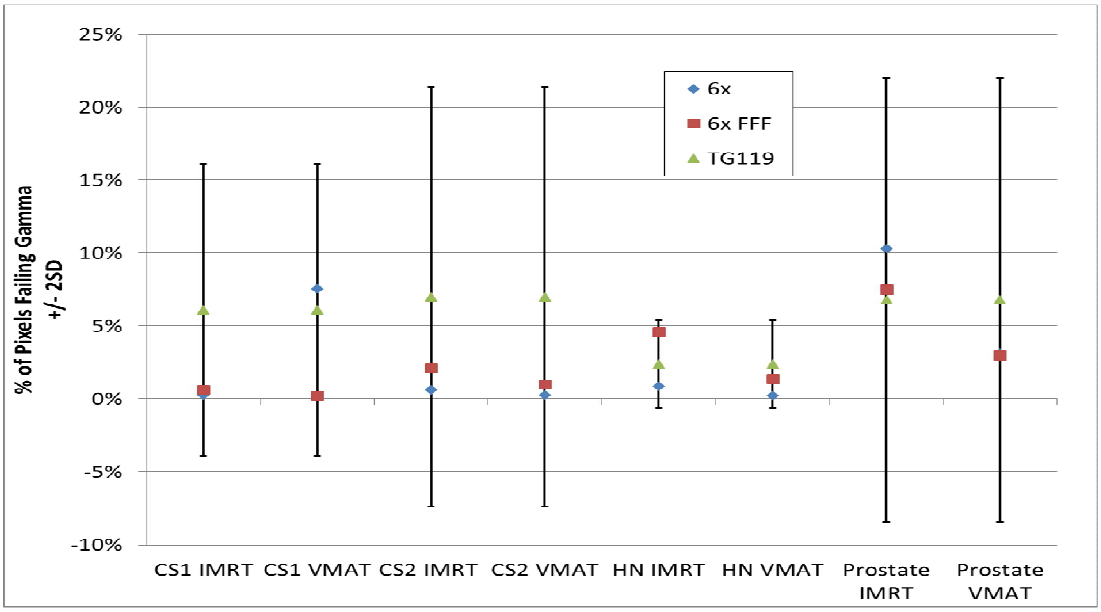

Figure 29: A low dose region comparison between film data for 6 MV, 6 MV FFF and TG119 institutions

b) Measured Data vs. TG119

Figure 30 shows a plan by plan comparison of the average error in the TG119 institutions. Inspection of these figures will show that our plans are comparable to those in TG119. Further, we calculated the confidence limit in a similar fashion to those regarding the ion chamber measurements, with the definition here being (CL = 100 - |mean|+1.96SD). The mean, in this case, is the percentage of points passing the gamma criteria. The compiled results for our study and the TG119 institutions are shown in Figure 31.

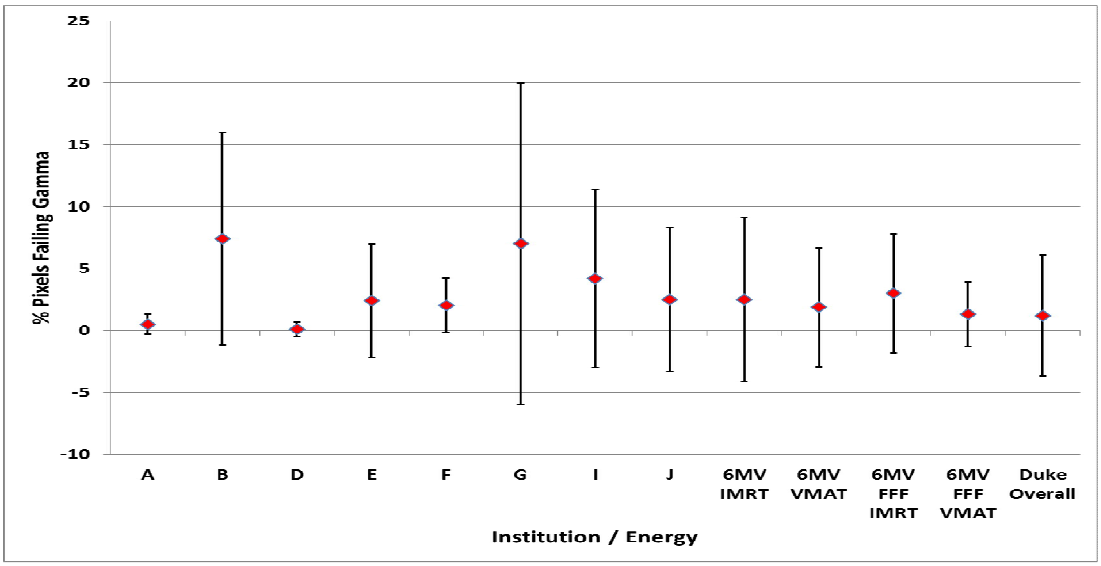

Figure 30: Mean % pixels failing gamma comparing TG119 institutions and measured data

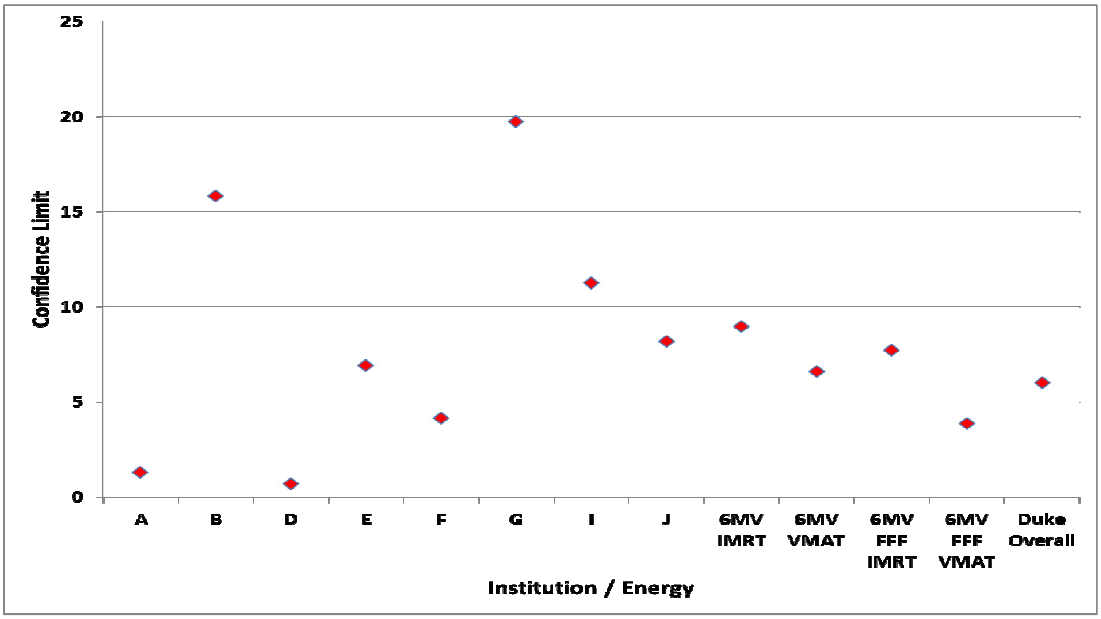

Figure 31: Confidence limit (% pixels failing gamma) comparing TG119 institutions and measured data

c) Statistical Analysis

Similar to the ion chamber analysis above, this is also testing the validity of the null hypothesis. The groups involved are 6 MV VMAT plans (FF and FFF) vs. 6 MV IMRT plans (FF and FFF), 6 MV FFF plans (VMAT and IMRT) vs. 6 MV FF plans (VMAT and IMRT), and 6 MV measurements in high dose regions (VMAT, IMRT, FF, and FFF plans) vs. low dose regions (VMAT, IMRT, FF, and FFF plans).We used the student's paired t-test comparing the fraction of points failing the gamma criteria in our plans, with the resulting p-values shown in Table 3.

Table 3: Statistical Differences for VMAT vs. IMRT, FFF vs. FF, and High vs. Low Dose Region 6MV Film Measurements Based on the Student's Paired T-Test

Tests	N (number of data pairs)	p-value	Statistically Significant
VMAT vs. IMRT	18	0.104	No
FFF vs. FF	18	0.922	No
High vs. Low	16	0.124	No

3.3.3. Delta4 Results

As an addition to the ion chamber and film measurements, we collected 3D dosimetric data for comparison.

a) Measured Dose vs. Planned Dose

Gamma parameters of 3% - 3mm with a 5% threshold were used (Table 4). All plans met acceptability criterion of 90% of pixels passing (average 99.7% +/- 0.8%). A second analysis was performed using 2%, 2mm gamma parameters (Table 5), where almost all plans met the 90% passing rate criteria (average 98.9% +/- 2.5%). The associated confidence limits are 1.9% failing (98.1% passing) for 3% DD, 3mm DTA and 6.0% failing (94% passing) for 2%, 2mm.

Table 4: Gamma 3%, 3 mm Passing Points Percentage for all Plans of all Energies

	6 MV	6 MV FFF	10 MV	10 MV FFF
Cshape 1 IMRT	100.0%	100.0%	100.0%	100.0%
Cshape 1 VMAT	99.9%	100.0%	100.0%	100.0%
Cshape 2 IMRT	100.0%	100.0%	100.0%	100.0%
Cshape 2 VMAT	100.0%	100.0%	99.9%	100.0%
H&N IMRT	99.6%	97.0%	98.2%	99.9%
H&N VMAT	100.0%	99.9%	100.0%	100.0%
MultiTarget IMRT	100.0%	100.0%	100.0%	100.0%
MultiTarget VMAT	99.7%	100.0%	100.0%	100.0%
Prostate IMRT	100.0%	100.0%	100.0%	100.0%
Prostate VMAT	100.0%	100.0%	100.0%	100.0%

“Real” H&N IMRT	98.3%	98.6%	98.4%	98.5%
“Real” H&N VMAT	96.7%	99.8%	100.0%	99.0%

Table 5: Gamma 2%, 2 mm Passing Points Percentage for all Plans of all Energies

	6 MV	**6 MV FFF**	**10 MV**	**10 MV FFF**
Cshape 1 IMRT	100.0%	99.9%	99.4%	99.8%
Cshape 1 VMAT	99.1%	100.0%	98.1%	99.7%
Cshape 2 IMRT	100.0%	99.8%	99.8%	99.5%
Cshape 2 VMAT	100.0%	100.0%	99.0%	99.9%
H&N IMRT	94.3%	95.2%	87.6%	91.5%
H&N VMAT	98.5%	99.8%	100.0%	99.7%
MultiTarget IMRT	100.0%	99.9%	99.9%	100.0%
MultiTarget VMAT	99.7%	98.2%	99.7%	99.5%
Prostate IMRT	100.0%	100.0%	100.0%	100.0%
Prostate VMAT	100.0%	100.0%	100.0%	100.0%
“Real” H&N IMRT	93.4%	96.5%	95.7%	96.6%
“Real” H&N VMAT	85.9%	94.5%	99.0%	91.9%

b) Measured Data vs. TG119

3D data was not collected by TG119, so no direct comparison can be made to its results. However, we used the confidence limit (CL) methodology of TG119 to calculate appropriate limits for our 3D dose measurements. To follow the ion chamber analysis, all calculations were done with and without the 10 MV H&N data.

Table 6: Confidence Limits (% Pixels Failing Gamma) for 3%, 3mm and 2%, 2mm Gamma Criteria

	3%, 3mm		2%, 2mm	
	Confidence Limit		Confidence Limit	
All Delta4 Measurements	1.9%		6.0%	
All Delta4 – 10 MV HN	1.8%		3.1%	
	6 MV	10 MV	6 MV	10 MV
All Delta4 Measurements	2.3%	1.4%	8.5%	8.3%
All Delta4 – 10 MV HN	2.3%	0.0%	8.5%	1.3%
	FF	FFF	FF	FFF
All Delta4 Measurements	2.0%	1.7%	9.8%	6.7%
All Delta4 – 10 MV HN	1.9%	1.7%	8.5%	4.2%
	IMRT	VMAT	IMRT	VMAT
All Delta4 Measurements	2.1%	1.6%	8.7%	8.0%
All Delta4 – 10 MV HN	1.9%	1.6%	5.3%	7.8%

c) Statistical Analysis

The validity of the standard null hypothesis was evaluated. The groupings were similar to those tested in Table 2. For example, the 6 MV VMAT vs. IMRT compares 6 MV VMAT plans (FF and FFF) vs. 6 MV IMRT plans (FF and FFF). We used the student's paired t-test comparing the fraction of points failing the gamma criteria in our plans, with the resulting p-values shown in Tables 7 and 8 on the following page. No statistically significant differences were observed.

Table 7: Statistical Differences for VMAT vs. IMRT and FFF vs. FF 3D Measurements Based on the Student's Paired T-Test

3%, 3 mm Gamma Analysis				
Energy	**N (Number of data pairs)**	**Tests**	**p-value**	**Statistically Significant**
6 MV	12	VMAT vs. IMRT	0.506	No
	12	FF vs. FFF	0.8	No
10 MV	12	VMAT vs. IMRT	0.116 (0.351 w/o HN)	No
	12	FF vs. FFF	0.669 (0.351 w/o HN)	No
6 MV & 10 MV	24	VMAT vs. IMRT	0.143 (0.514 w/o 10 MV HN)	No
	24	FF vs. FFF	0.668 (0.777 w/o 10 MV HN)	No

Table 8: Statistical Comparison of 2% / 2mm Gamma Analysis of 3D Data

2%, 2 mm Gamma Analysis				
Energy	**N (Number of data pairs)**	**Tests**	**p-value**	**Statistically Significant**
6 MV	12	VMAT vs. IMRT	0.76	No
	12	FF vs. FFF	0.182	No
10 MV	12	VMAT vs. IMRT	0.318 (0.143 w/o HN)	No
	12	FF vs. FFF	0.991 (0.211 w/o HN)	No
6 MV & 10 MV	24	VMAT vs. IMRT	0.492 (0.586 w/o 10 MV HN)	No
	24	FF vs. FFF	0.321 (0.112 w/o 10 MV HN)	No

d) Delta4 vs. Film

We used the Pearson Correlation Coefficient and Spearman's Rho calculations to determine if the film and Delta4 results were correlated (Table 9). The Pearson Correlation Coefficient is used to estimate the strength of a linear relationship between two variables. Spearman's Rho, on the other hand, estimates the strength of a monotonic relationship between two variables. For both tests, r = +/-1 would be a perfect positive/negative correlation.

All tests showed a weak positive correlation between the data. A plan-by-plan comparison is displayed in Figure 32 below.

Table 9: Film – Delta4 Data Correlation

	Pearson Correlation Coefficient (r)	Spearman's Rho (R)
Film (3%, 3mm) vs. Delta4 (3%, 3mm)	0.440	0.462
Film (3%, 3mm) vs. Delta4 (2%, 2mm)	0.200	0.403

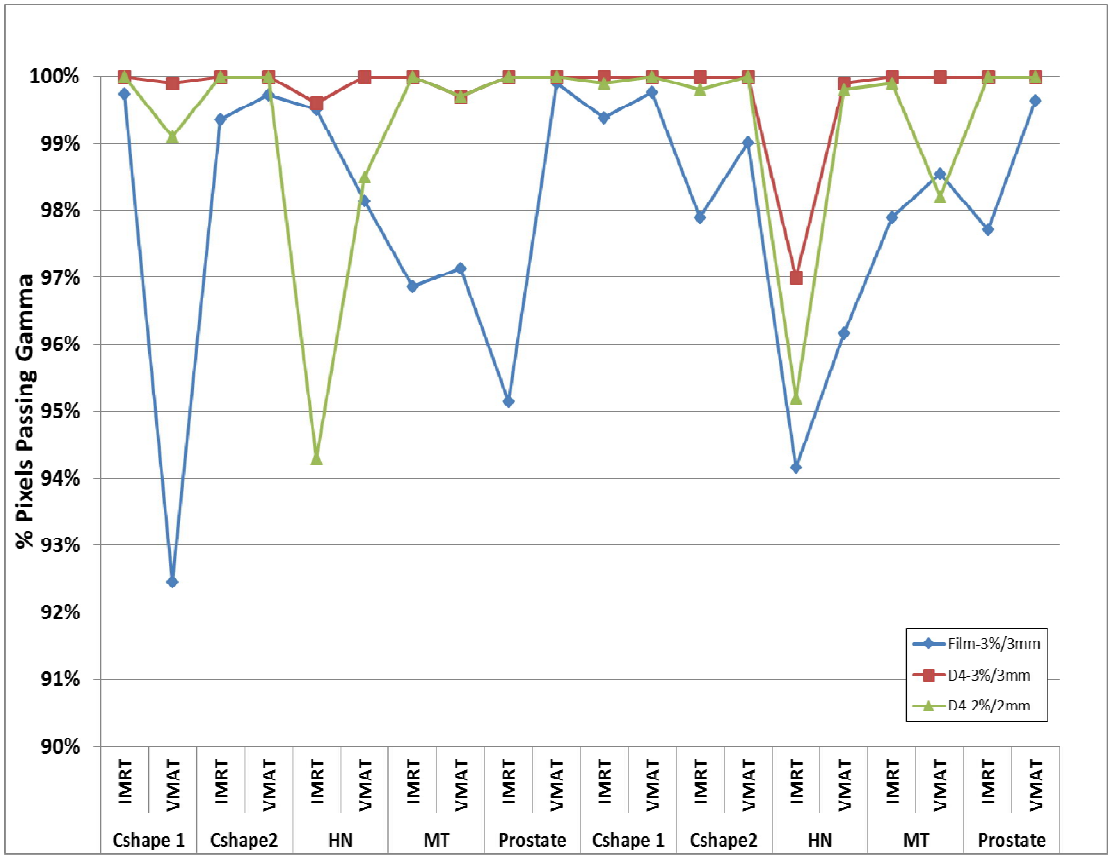

Figure 32: Correlation between film results and Delta4 results

3.4. P_{ion} Effect

The ion recombination correction factor (P_{ion}) corrects for the loss of ions in the chamber due to the general recombination, initial recombination and diffusion against the electric field [11]. P_{ion} can be measured by taking readings at two different bias voltages and the ratio of the readings lead to P_{ion} [13].

$$P_{ion} = (1 - V_H / V_L) / (M_H / M_L - V_H / V_L) \quad [14]$$

In the above equation, V_H is the operating voltage and V_L is half of V_H; M_H and M_L are the raw ion chamber readings at V_H and V_L.

Wang et al. showed that the removal of the Flattening Filter can affect the ion recombination in the ion chamber [15]. This effect can be due to the increased dose rate, the main advantage of the Flattening Filter Free mode. We studied the difference between using the flattened beam versus the softer flattening filter free one on the P_{ion}.

Given that the recombination effect is a function of dose per pulse (MU/min), we tested the effect on a FFF beam by comparing P_{ion} for 6 MV to 6 MV FFF at the isocenter. We delivered 200 MUs in each measurement and set the field size to 10x10 cm^2 and 100 cm SSD. Table 10 shows the P_{ion} values for 6 MV and 6 MV FFF with the chamber at various depths.

This test showed an insignificant difference between the P_{ion} for 6 MV FF and 6 MV FFF beams (less than 0.5%), in agreement with Wang's results. Wang studied the variation in P_{ion} between flat and FFF beams for 6 MV and 10 MV using three different

chambers. They used an SAD setup with a chamber depth of 10 cm and field size of 10x 10 cm^2. They reported that all measured P_{ion} fell between 1% and 1.02 % [15].

Table 10: P_{ion} Values for 6 MV and 6 MV FFF with the Chamber Inserted in Different Depths

Depth (cm)	6 MV P_{ion}	6 MV FFF P_{ion}
1.5	1.006	1.004
7.5	1.009	1.005
15.0	1.008	1.007

3.5. High Dose Rate Effect

The main advantage of having a flattening filter free beam is the availability to treat using very high dose rates, which results in a shorter treatment time. We compared our ion chamber and Delta4 measurements for 6 MV FFF with dose rates from 400 MU/min to 1400 MU /min and the results were comparable to each other. These results are similar to published findings [16].

We chose a 6 MV FFF TG119 HN IMRT case to conduct this test. We tested the effect of high dose rate by gradually increasing the dose rate from 600 MU/min to 1400 MU/min, and then took measurements using the cc01 ion chamber. We also took Delta4 measurements for the same dose rates and the results were identical through the different dose rates. The ion chamber's percentage difference is shown in Table 11.

Table 11: Ion Chamber Measurement vs. Planned Results

Dose Rate (MU/min)	% Difference
600	0.1%
1000	-0.3%
1200	-0.4%
1400	-0.6%

4. Discussions

4.1. Planning Results

From the data in Tables A through D in Appendix A, we found that all IMRT plans and most of the VMAT plans achieved the TG119 planning goals within two standard deviations of the TG119 institutions. The four goals in FFF VMAT plans that did not meet the criterion are: 6 MV FFF Cshape (easy), where we noticed that D10 for both PTV and the core are too high; D10 of the core in Cshape (hard) is also much higher than the goal; and D20 is much higher than the TG119 goal in the ”real” HN case. The “real” HN case was not compared to TG119 institutions since they did not have a similar case.

4.2. Bands Results

The bands results of 98.81% and 98.90% for 6 MV and 6 MV FFF which suggests that our film processor/scanner system is acceptable. These results fall within the range of the four TG119 institutions that submitted the gamma passing rates for their bands film measurements.

4.3. Test Cases

4.3.1. Ion Chamber

The majority (94%) of ion chamber measurements passed an acceptance criterion of +/-3% agreement with the planned dose, indicating that all energies and modalities tested were adequately commissioned. This result supports our first hypothesis, that

TG119 methodology may be used for commissioning VMAT and FFF in addition to the traditional IMRT and FF. Measurements that failed both Duke and TG119 acceptance criteria were associated with a site/energy combination (10 MV for HN plans) that would not be clinically used. For that challenging situation, VMAT provided better agreement with planned doses than IMRT, perhaps because of the greater degrees of freedom offered by a double-arc beam arrangement. Switching to a "real" HN case instead of the TG119 clinical case provided more forgiving geometry, enabling an improved agreement between 10 MV planned and measured doses. Our clinical recommendation is to restrict TG119 testing to site/energy/delivery technique combinations that will be in clinical use.

The confidence limits calculated from our measurements are generally in good agreement with the +/-3% acceptance criterion when the 10 MV HN data is removed. The measured results are biased by pre-knowledge of that criterion, such that any measurements with errors >3% were re-measured while measurements within 3% typically were not. The 6 MV and 10 MV confidence limits were similar (3.5% & 3.3%), indicating a similar measurement uncertainty. The IMRT and VMAT confidence limits (3.3% & 2.9%) were likewise similar. More uncertainty was seen with FFF (4.0%) than FF (2.8%). Measurements in the low dose region (2.7%) had less uncertainty than in the high dose region (3.4%), because the error was calculated relative to the prescription

dose rather than the local dose. The larger absolute dose differences possible in the high dose region increase its uncertainty.

In general, the difference in ion chamber measurements for IMRT vs. VMAT, FFF vs. FF, and high dose region vs. low dose region were statistically insignificant. FFF vs. FF was statistically significant, but only for 6 MV (average error: -0.9% vs. -0.2%). The difference is larger when only 6 MV IMRT plans are evaluated ($p = 0.0018$, average error: 1.3% FFF vs. -0.2% FF). There were no statistically significant differences between FF and FFF with either the 10 MV data or the combined energy data. This indicates that the difference may originate in the modeling of the 6 MV FFF beam or in some interaction of a FFF delivery with a low energy beam causing higher uncertainty. While VMAT vs. IMRT with combined energies is statistically significant, the significance disappears with the 10 MV HN case is removed. The lack of statistically significant differences between VMAT/IMRT and FF/FFF measurements supports the hypothesis that TG119 methodology is appropriate for commissioning VMAT & FFF. The difference between high and low dose measurements was statistically significant as expected, for the same reason discussed above: calculating the error relative to the prescription dose rather than the local dose.

4.3.2. Film

All film planes met the acceptability criterion of <= 10% of pixels failing 3%, 3mm gamma. Our passing rates were typically equal to or better than those reported in TG119. The overall TG119 film confidence limit was 12.4% of pixels failing, compared to our measured confidence limit of 6% of pixels failing. These results indicate a successful commissioning of VMAT/IMRT and FF/FFF modes for the 6 MV energy at Duke. No statistically significant differences were found between VMAT/IMRT, FF/FFF, and high/low dose regions. The film results support the hypothesis that TG119 methodology may be used for commissioning VMAT and FFF.

4.3.3. Delta4

Part of the challenge of analyzing 3D dose measurements is the determination of appropriate gamma criteria. In this analysis we have examined both 3%, 3mm and 2%, 2mm criteria. The passing rates with 3%, 3mm were very high for all films. While this indicates that all energies/modalities were adequately commissioned, it does not allow us to separate out the hard-to-achieve plans from the easy-to-achieve plans. Using 2%, 2mm criterion provides us with more information for analysis. The detrimental impact of including 10 MV HN plans is clear (6% confidence level with 10 MV HN plans vs. 3% without). The 6 MV and 10 MV confidence limits appear very different when the 10 MV HN plans are removed (8.5% vs. 1.3%), but we believe that is due to removing the hardest-to-achieve plans (HN) from the 10 MV energy analysis while leaving them in the

6 MV energy analysis. With all HN plans included, there is no difference in the confidence limit between 6 MV and 10 MV. While not statistically significant, the passing rates were higher for FFF than FF plans, indicating that the new FFF technology was adequately commissioned. There was no statistically significant difference between IMRT and VMAT plans. These results support the hypothesis that TG119 methodology is appropriate for commissioning VMAT and FFF.

We included the Delta4 3D dose measurements in this study because many clinics no longer have the ability to measure 2D film data. Could Delta4 be used to replace film measurements for commissioning? Unfortunately, no clear correlation was found between film and Delta4 data. While some plans had lower passing rates for both film and Delta4 (e.g. 6 MV FFF IMRT HN) others had a dramatically lower passing rate for one modality but not the other (e.g. 6 MV IMRT Prostate). Our data do not support replacing film with Delta4 (3D) measurements, disproving our second hypothesis. Ideally a clinic would use both technologies for the most complete evaluation.

5. Conclusions

The results show that TG119 can be used to test in commissioning IMRT and VMAT delivery techniques and of Flattening-Filter and Flattening-Filter-Free modes. The commissioning of 6 MV/10 MV, IMRT/VMAT, FF/FFF beam combinations was verified using ion chamber (point measurement), film (2D) and multi-planar diode (Delta4, 3D) measurements.

Confidence limits were established for ion chamber (3.1%), film (6%), and Delta4 (3.1%) measurements. All the confidence limits were comparable to TG119 institutions. We recommend that non-clinical plans (e.g. 10 MV HN plans) not be included in TG119 evaluations. We also recommend that film continue to be used as the gold standard of multi-dimensional measurements, rather than be replaced by diode-based technology.

Appendix A

Table A: 6 MV with FF TrueBeam Planning Results

Plan	Goal(s)	TG119-Planning IMRT (Gy)	TG119-Planning VMAT (Gy)	TG119 mean + SD	Achieved within 2SD
MultiTarget	Central target D99 > 50Gy	49.98	49.99	49.55 ± 1.62	Yes
	Central target D10 < 53Gy	52.93	54.03	54.55 ± 1.73	Yes
	Superior target D99 > 25Gy	25.07	24.62	25.16±0.85	Yes
	Superior target D10 < 35Gy	32.05	33.31	34.12±3.04	Yes
	Inferior target D99 > 12.5Gy	13.26	14.07	14.07±1.85	Yes
	Inferior target D10 < 25Gy	23.78	24.24	24.18±2.72	Yes
Prostate	Prostate D95 > 75.6Gy	75.60	75.59	75.66±0.21	Yes
	Prostate D5 < 83Gy	79.34	79.75	81.43±1.56	Yes
	Rectum D30 < 70Gy	64.29	66.88	65.36±2.97	Yes
	Rectum D10 < 75Gy	72.34	74.50	73.03±1.5	Yes
	Bladder D30 < 70Gy	40.08	43.68	43.94±8.78	Yes
	Bladder D10 < 75Gy	59.82	61.82	62.69±8.15	Yes
H&N-TG119	PTV D90 = 50Gy	50.00	49.18	50.28±0.58	Yes
	PTV D99 > 46.5Gy	47.97	47.50	47.04±0.52	Yes
	PTV D20 < 55Gy	52.19	53.26	52.99±0.93	Yes
	Cord max < 40Gy	39.19	38.89	37.41±2.50	Yes
	Parotid D50 < 20Gy	18.36	18.07	17.98±1.84	Yes

Cshape (easy)	PTV D95 = 50Gy	49.98	50.00	50.1±0.17	Yes
	PTV D10 < 55Gy	53.6	54.57	54.4±0.52	Yes
	Core D10 < 25Gy	22.32	24.16	22±3.14	Yes
Cshape (hard)	PTV D95 = 50Gy	49.99	49.99	50.11±0.165	Yes
	PTV D10 < 55Gy	56.22	58.02	57.02±2.2	Yes
	Core D10 < 10Gy	14.59	16.30	16.3±3.07	Yes
H&N- ″real″	PTV D90 = 50Gy	52.09	51.28	n/a	n/a
	PTV D99 > 46.5Gy	49.54	49.42	n/a	n/a
	PTV D20 < 55Gy	54.64	53.38	n/a	n/a
	Cord max < 40Gy	23.73	23.63	n/a	n/a
	Lt Parotid D50 < 20Gy	15.62	18.49	n/a	n/a
	Rt Parotid D50 < 20Gy	15.32	17.56	n/a	n/a

Table B: 6 MV FFF TrueBeam Planning Results

Plan	Goal(s)	Planning IMRT (Gy)	Planning VMAT (Gy)	TG119 mean + SD	Achieved within 2SD
MultiTarget	Central target D99 > 50Gy	49.98	49.99	49.55 ± 1.62	Yes
	Central target D10 < 53Gy	53.27	54.58	54.55 ± 1.73	Yes
	Superior target D99 > 25Gy	24.64	24.71	25.16±0.85	Yes
	Superior target D10 < 35Gy	31.55	33.72	34.12±3.04	Yes
	Inferior target D99 > 12.5Gy	12.53	14.14	14.07±1.85	Yes
	Inferior target D10 < 25Gy	22.52	24.52	24.18±2.72	Yes
Prostate	Prostate D95 > 75.6Gy	75.59	75.59	75.66±0.21	Yes
	Prostate D5 < 83Gy	79.56	80.02	81.43±1.56	Yes
	Rectum D30 < 70Gy	64.20	66.88	65.36±2.97	Yes
	Rectum D10 < 75Gy	72.43	74.53	73.03±1.5	Yes
	Bladder D30 < 70Gy	39.83	43.86	43.94±8.78	Yes
	Bladder D10 < 75Gy	58.77	61.84	62.69±8.15	Yes
H&N	PTV D90 = 50Gy	50.00	49.95	50.28±0.58	Yes
	PTV D99 > 46.5Gy	47.89	47.51	47.04±0.52	Yes
	PTV D20 < 55Gy	52.06	53.43	52.99±0.93	Yes
	Cord max < 40Gy	39.26	39.24	37.41±2.50	Yes
	Parotid D50 < 20Gy	17.69	16.93	17.98±1.84	Yes
Cshape	PTV D95 =	49.99	50.02	50.1±0.17	Yes

(easy)	50Gy				
	PTV D10 < 55Gy	53.82	65.71	54.4±0.52	Yes IMRT / NO VMAT
	Core D10 < 25Gy	21.49	63.35	22±3.14	Yes IMRT / NO VMAT
Cshape (hard)	PTV D95 = 50Gy	49.98	49.99	50.11±0.165	Yes
	PTV D10 < 55Gy	56.44	60.50	57.02±2.2	Yes
	Core D10 < 10Gy	14.24	32.81	16.3±3.07	Yes IMRT / NO VMAT
H&N- ″real″	PTV D90 = 50Gy	52.09	49.99	n/a	n/a
	PTV D99 > 46.5Gy	49.43	46.28	n/a	n/a
	PTV D20 < 55Gy	54.97	58.78	n/a	n/a
	Cord max < 40Gy	23.42	23.28	n/a	n/a
	Lt Parotid D50 < 20Gy	15.43	15.21	n/a	n/a
	Rt Parotid D50 < 20Gy	15.09	17.93	n/a	n/a

Table C: 10 MV with FF TrueBeam Planning Results

Plan	Goal(s)	Planning IMRT (Gy)	Planning VMAT (Gy)	TG119 mean + SD	Achieved within 2SD
MultiTarget	Central target D99 > 50Gy	49.77	49.98	49.55 ± 1.62	Yes
	Central target D10 < 53Gy	54.00	54.90	54.55 ± 1.73	Yes
	Superior target D99 > 25Gy	24.88	24.46	25.16±0.85	Yes
	Superior target D10 < 35Gy	32.21	33.81	34.12±3.04	Yes
	Inferior target D99 > 12.5Gy	13.08	13.91	14.07±1.85	Yes
	Inferior target D10 < 25Gy	23.44	25.02	24.18±2.72	Yes
Prostate	Prostate D95 > 75.6Gy	75.59	75.59	75.66±0.21	Yes
	Prostate D5 < 83Gy	79.81	79.52	81.43±1.56	Yes
	Rectum D30 < 70Gy	64.75	67.01	65.36±2.97	Yes
	Rectum D10 < 75Gy	72.8	74.82	73.03±1.5	Yes
	Bladder D30 < 70Gy	39.72	42.19	43.94±8.78	Yes
	Bladder D10 < 75Gy	59.68	60.98	62.69±8.15	Yes
H&N	PTV D90 = 50Gy	50.00	49.91	50.28±0.58	Yes
	PTV D99 > 46.5Gy	48.32	47.36	47.04±0.52	Yes
	PTV D20 < 55Gy	51.86	53.10	52.99±0.93	Yes
	Cord max < 40Gy	39.42	38.84	37.41±2.50	Yes
	Parotid D50 < 20Gy	20.12	18.68	17.98±1.84	Yes

Cshape (easy)	PTV D95 = 50Gy	49.98	50.00	50.1±0.17	Yes
	PTV D10 < 55Gy	52.68	54.92	54.4±0.52	Yes
	Core D10 < 25Gy	24.76	24.99	22±3.14	Yes
Cshape (hard)	PTV D95 = 50Gy	49.99	50.00	50.11±0.165	Yes
	PTV D10 < 55Gy	53.39	58.25	57.02±2.2	Yes
	Core D10 < 10Gy	21.46	17.13	16.3±3.07	Yes
H&N- ″real″	PTV D90 = 50Gy	52.02	53.04	n/a	n/a
	PTV D99 > 46.5Gy	49.72	48.93	n/a	n/a
	PTV D20 < 55Gy	54.48	56.34	n/a	n/a
	Cord max < 40Gy	24.55	24.88	n/a	n/a
	Lt Parotid D50 < 20Gy	17.25	18.95	n/a	n/a
	Rt Parotid D50 < 20Gy	16.55	17.26	n/a	n/a

Table D: 10 MV FFF TrueBeam Planning Results

Plan	Goal(s)	Planning IMRT (Gy)	Planning VMAT (Gy)	TG119 mean + SD	Achieved within 2SD
MultiTarget	Central target D99 > 50Gy	49.99	49.98	49.55 ± 1.62	Yes
	Central target D10 < 53Gy	53.86	54.90	54.55 ± 1.73	Yes
	Superior target D99 > 25Gy	24.70	24.73	25.16±0.85	Yes
	Superior target D10 < 35Gy	32.73	33.96	34.12±3.04	Yes
	Inferior target D99 > 12.5Gy	13.01	13.95	14.07±1.85	Yes
	Inferior target D10 < 25Gy	23.78	23.17	24.18±2.72	Yes
Prostate	Prostate D95 > 75.6Gy	75.58	75.58	75.66±0.21	Yes
	Prostate D5 < 83Gy	80.10	79.69	81.43±1.56	Yes
	Rectum D30 < 70Gy	64.78	67.30	65.36±2.97	Yes
	Rectum D10 < 75Gy	72.85	74.70	73.03±1.5	Yes
	Bladder D30 < 70Gy	40.37	43.32	43.94±8.78	Yes
	Bladder D10 < 75Gy	61.08	62.98	62.69±8.15	Yes
H&N	PTV D90 = 50Gy	50.00	49.93	50.28±0.58	Yes
	PTVD99 > 46.5Gy	48.16	47.34	47.04±0.52	Yes
	PTV D20 < 55Gy	51.89	53.34	52.99±0.93	Yes
	Cord max < 40Gy	39.22	39.04	37.41±2.50	Yes
	Parotid D50 < 20Gy	18.83	17.77	17.98±1.84	Yes
Cshape (easy)	PTV D95 = 50Gy	50.00	49.97	50.1±0.17	Yes

	PTV D10 < 55Gy	53.44	55.52	54.4±0.52	Yes
	Core D10 < 25Gy	25.29	24.50	22±3.14	Yes
Cshape (hard)	PTV D95 = 50Gy	50.00	49.93	50.11±0.165	Yes
	PTV D10 < 55Gy	53.73	58.35	57.02±2.2	Yes
	Core D10 < 10Gy	18.53	15.56	16.3±3.07	Yes
H&N- ″real″	PTV D90 = 50Gy	52.05	49.98	n/a	n/a
	PTV D99 > 46.5Gy	49.57	45.55	n/a	n/a
	PTV D20 < 55Gy	54.71	64.06	n/a	n/a
	Cord max < 40Gy	23.88	23.17	n/a	n/a
	Lt Parotid D50 < 20Gy	16.24	17.64	n/a	n/a
	Rt Parotid D50 < 20Gy	15.46	15.76	n/a	n/a

References

[1] Van Dyk, The Modern Technology of Radiation Oncolgy, Madison, Wisconsin: Medical Physics Publishing, 1999.

[2] Ezzell, Burmeister, Dogan, et al., "IMRT commissioning: Multiple institution planning and dosimetry comparisons, a report from AAPM Task Group 119" Med Phys (36), pp. 5359-5373, 2009.

[3] Cashmore, "The characterization of unflattened photon beams from a 6 MV linear accelerator" Phys Med Biol (53), pp. 1933 - 1946, 2008.

[4] Chandraraj, Stathakis, Manickam, et al. "Comparison of four commercial devices for RapidArc and sliding window IMRT QA" J Appl Clin Med Phys (11), 2011.

[5] Mynampati, Yaparpalvi, Hong, et al., "Application of AAPM TG119 to volumetric arc therapy (VMAT)" J Appl Clin Med Phys (13), pp. 108 - 116, 2012.

[6] Ling, Zhang, Archambault, et al., "Commissioning and Quality Assurance of RapidArc Radiotherapy Delivery System" Int J Radiat Oncol Biol Phys (72), pp. 575 - 581, 2008.

[7] Bedford, Warrington, "Commissioning of volumetric modulated arc therapy (VMAT)" Int J Radiat Oncol Biol Phys (73), pp. 537 - 545, 2009.

[8] Ezzell, Galvin, Low, et al., "Guidance document on delivery, treatment planning, and clinical implementation of IMRT: Report of the IMRT subcommittee of the AAPM radiation therapy committee" Med Phys (30), pp. 2089 - 2115, 2003.

[9] Ting, "Facts and Fictions of Flattening Filter Free (FF-FFF) X-Rays Beams" Med. Phys. (39), pp. 3861, 2012 .

[10] Sharma, "Unflattened photon beams from the standard flattening filter free accelerators for radiotherapy: Advantages, limitations and challenges" J Med Phys. (36), pp. 123 - 125, 2011.
http://www.ncbi.nlm.nih.gov/pmc/articles/PMC3159217/

[11] Podgorsak, Radiation Oncolgy Physics: A Handbook for Teachers and Students, Vienna: International Atomic Energy Agency, 2005.

[12] Kragl, af Wetterstedt, Knausl, et al. "Dosimetric characteristics of 6 and 10 MV unflattened photon beams" Radiother Oncol (93), pp. 141 - 146, 2009.

[13] Khan, The Physics of Radiation Therapy, Philadelphia: Lippincott Williams & Wilkins, 2003.

[14] Almond, Biggs, Coursey, et al. "AAPM's TG-51 protocol for clinical reference dosimetry of high-energy photon and electron beams" Med Phys (26), pp. 1847 - 1870, 1999.

[15] Wang, Easterling, Ting, "Ion recombination corrections of ionization chambers in flattening filter-free photon radiation" J Appl Clin Med Phys (13) , pp. 262-268, 2012.

[16] Kalantzis, Qian, Han, et al., "Fidelity of dose delivery at high dose rate of volumetric modulated arc therapy in a truebeam linac with flattening filter free beams" J Med Phys (37), pp. 193-199, 2012.
http://www.ncbi.nlm.nih.gov/pubmed/23293450

[17] Lohse, Lang, Hrbacek, et al., "Effect of high dose per pulse flattening filter-free beams on cancer cell survival" Radiother Oncol (101), pp. 226 - 232, 2011.

[18] Kretschmer, Sabatino, Blechschmidt, et al., "The impact of flattening-filter-free beam technology on 3D conformal RT" Radiat Oncol (8), 2013.

[19] Sathiyan, Ravikumar, Boyer, et al., "Comparison of IMRT and RapidArctreatment plans using AAPM task group test suites" Gulf J Oncol (10), pp. 11-17, 2011.
http://www.ncbi.nlm.nih.gov/pubmed/21724524

[20] Feygelman, Zhang, Stevens, et al., "Evaluation of a new VMAT QA device, or the "X" and "O" array geometries" J Appl Clin Med Phys (12), pp. 146 – 168, 2011.

[21] Gordon, Krafft, Jang, et al., "Confidence limit variation for a single IMRT system following the TG119 protocol" Med Phys (38), pp. 1641 - 1648, 2011.

[22] Saminathan, Manickam, Chandraraj, "Plan evaluation and dosimetric comparison of IMRT using AAPM TG119 test suite and recommendations" Australas Phys

Eng Sci Med (34), pp. 55-61, 2011.

[23] Feygelman, Zhang, Stevens, "Initial dosimetric evaluation of SmartArc - a novel VMAT treatment planning module implemented in a multi-vendor chain" J Appl Clin Med Phys (11), p. 99, 2010.

[24] Low, Harms, Mutic, et al., "A technique for the quantitative evaluation of dose distributions" Med Phys (25), pp. 656 - 661, 1998.

[25] Venselaar, Welleweerd, Mijnheer, "Tolerance for the accuracy of photon beam dose calculations of treatment planning systems" Radiother Oncol (60), pp. 191 - 201, 2001.

[26] P Mayles, A Nahum and J C Rosenwald. 2007. *Handbook of Radiotherapy Physics, Theory and Practice.* New York London : Taylor & Francis Group, LLC, 2007.